

The Alpi Linac as RNB Accelerator

8.1 Introduction

The superconducting linac ALPI, available at present for stable beams injected either by an XTU Tandem ($V_T = 15$ MV) or by PIAVE (composed by an ECR ion source on a HV platform, followed by 2 superconducting RFQs and 8 Quarter Wave resonators), will serve as the accelerator of exotic species produced in the target-ion-source system, transported through the long transport line hosting the beam cooler and the high resolution mass separator and charge bred in the charge breeder (CB) of the ECR Ion Source type.

In order to be adapted to SPES, ALPI shall have to be equipped with a new injector, starting with the CB ion source.

The CB will be the first element along the beam line of the RNB ALPI injector, and will be followed by a long normal conducting RFQ working in the CW mode and by a transport line. The latter matches the beam for the linac injection both transversally (by magnetic quadrupole lenses) and longitudinally, i.e. in time and phase, by means of an appropriate number of bunching cavities. Injection into ALPI will take place at a 0° entrance into dipole ID2, which presently bends the beam, coming from the tandem injector, into the linac.

The layout of the SPES facility, with a zoom on the new injection line, is shown in fig. 8.1.

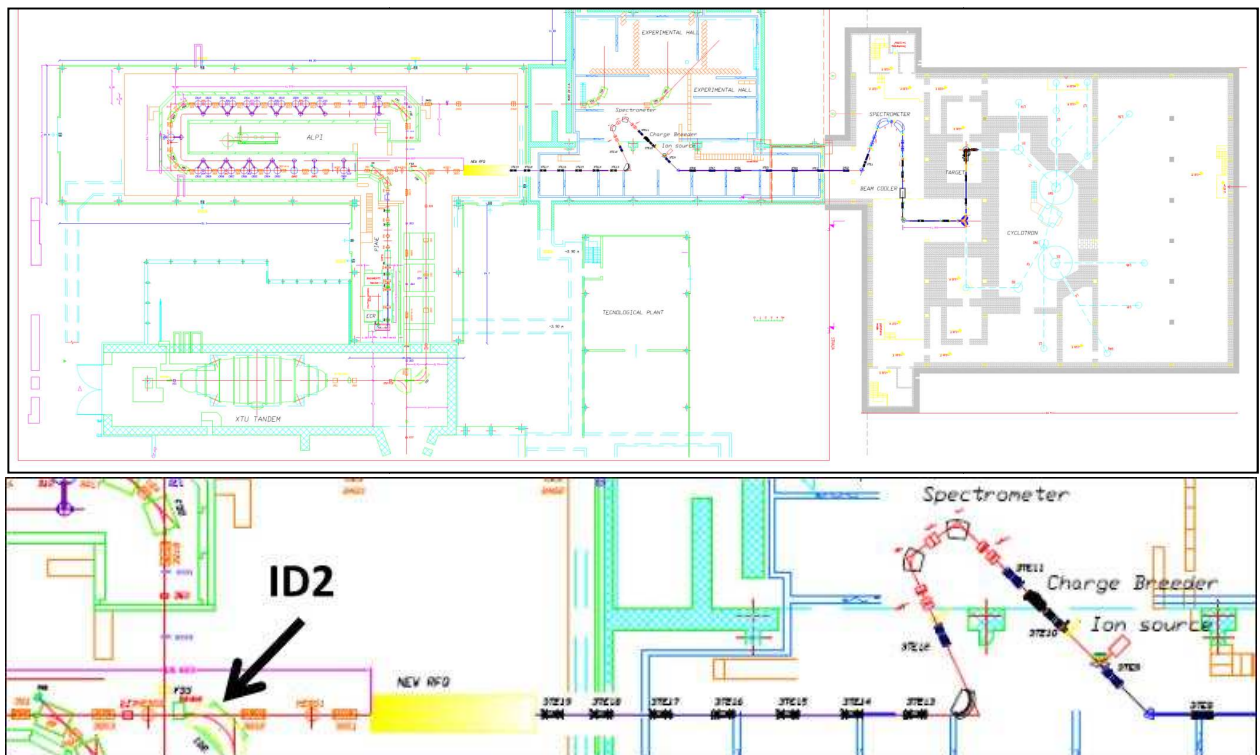


Figure 8.1: Layout of the SPES facility, and zoom on the Charge Breeder and the downstream spectrometer and RFQ (new RNB injector into the ALPI superconducting linac)

Within ALPI itself, some modifications or upgrades are necessary in order both to make the linac suitable to the acceleration and transport of a RNB up to the desired final energy and overall beam transmission. They are listed hereinafter, together with other changes required on

some obsolete technical features of ALPI in order to ensure reliable operation, for both radioactive and stable beams, in the next couple of decades:

1. The so called “low beta section” (comprising originally 12 resonators with an operational accelerating field $E_a < 3,5$ MV/m) is being changed into 16 resonators with $E_a = 5$ MV/m at least, which will improve the acceleration efficiency of the rest of the linac, the beam final energy and transmission (in the longitudinal phase space ΔE - Δt)

2. New quadrupoles with a higher gradient (25 vs. 20 T/m) are in principle required in ALPI, in order to increase the overall beam transmission

3. Beyond what is achieved by the upgrade of lower beta section (point 1 above), substantial increase in the final energy of the beam can be obtained by adding two cryostats with Nb-sputtered cavities at the very end of the linac; this can be the result of a reshuffling of cryostats in ALPI, i.e. moving the present bunching cavity cryostat CRB2 towards position CR21 and the present rebunching/debunching cryostat CRB4 to position CR22; one normal conducting cavity at the beginning of ALPI and one single-cavity SC re/debuncher at the end of ALPI will replace them;

4. Beam diagnostics for low-intensity beams must be integrated with that for stable beams, if possible in the space allocated for the diagnostics boxes available at present.

5. Cryogenics operations: the new ALPI layout foresees relocating PIAVE cryostats CR01-P and CR02-P to positions CR01 and CR02 in ALPI, which can be done by adapting the cryogenic lines in that area; the available cryogenic power of ALPI has been recently increased by around 30% with the addition of a 3rd turbine; cryostats and the cryo-plant need a modernization of their control system; cryo-module feedboxes need to be stepwise replaced with new ones with external actuators; the compressor section of the cryogenic plant requires a number of important refurbishment steps.

6. Control systems: nearly all of them must be partly or completely upgraded (e.g. RF, diagnostics, magnets, access) and their hardware changed.

7. Vacuum system: a replacement of most vacuum and fore vacuum pumps is required, dictated both by the ageing of ALPI ones and by the necessity to use pumps suitable for radioactive contaminants; in addition, is necessary to conveying all the exhaust residues into a controlled outlet, and, according to radioprotection requirements, to define time and criteria of their delivery.

In the following paragraphs, all above implementations, upgrades and refurbishments shall be reviewed. At the date of the present document, their development stage is diversified, which is due to the fact that SPES is a new facility which is, however, developed into an existing one (the Tandem-ALPI-PIAVE stable beam complex).

Paragraph 2 describes the charge breeding source, i.e. the first element of the new injector; paragraph 3 is dedicated to the overall beam dynamics and includes the remaining part of the injector and, in particular, the normal conducting RFQ, the longitudinal focusing system with new normal conducting bunchers, the transverse focusing system with higher gradient quadrupoles in the low-energy branch, the relocated PIAVE cryostats and the relocated ALPI bunching cryostats, used for further beam acceleration; paragraph 4 describes, in more detail, the upgrade of the low beta section of ALPI (involving cryostats CR03 to CR06) while paragraph 5 deals with the energy upgrade, obtained by relocating the present bunching cryostats as accelerating cryostats at the end of the linac; in paragraph 6, the diagnostics systems necessary

along the whole beam line from the target-ion-source to the end of ALPI are drafted (R&D activity is on-going on this issue); in paragraph 7, finally, upgrades and refurbishment of the cryogenic plant are described.

8.2 The Charge Breeder

8.2.1 Introduction

After passing the High Resolution Mass Spectrometer (HRMS), the radioactive beam will be cleaned from contaminants and will be ready for post-acceleration. Anyway, a charge state 1+ is too low to have a reasonable energy for the experiments after the acceleration with the new RFQ coupled to the superconducting linac ALPI (linac beta profile). For this reason, a further device has to be implemented, able to accept a 1+ beam, to multiply its charge state and to extract it as an n+ beam. This work is done by the so called "Charge Breeder" (CB). The charge breeding technique was extensively studied in the past years; basically, three methods were developed so far as described in [1].

8.2.2 Charge Breeding Methods

The first method consists simply in stripping electrons by means of a foil or a gas. When the foil is used it is possible to predict the charge state distribution after the stripper by using the Baron's formula giving the output average charge state [1]. This is seen to depend on the velocity of the incoming beam and its atomic number. This technique gives a narrow charge state distribution for low Z elements but a wider one for high Z, leading to a low efficiency on a single charge state. Moreover, the incoming beam energy has to be at least 500 keV/A, much higher than that of the 1+ beam (40 keV of total energy) coming from the Target-Ion Source system of the SPES project. Lower energy would be sufficient if a gas stripper was used but the output charge states would be very low. Other drawbacks of this method are the increase of the emittance of the incoming beam after passing the stripper and the limited lifetime of the foils in case of heavy elements.

The other two methods consist in adapting an ion source for positive ion beams production to the charge breeding technique. In particular two kinds of ion sources are used to this purpose: the Electron Beam Ion Sources (EBIS) and the Electron Cyclotron Resonance Ion Sources (ECRIS). In an EBIS [2] multicharged ions are produced ionizing the incoming beam by collisions with an electron beam compressed by a solenoid magnetic field and trapped in a magneto-electrostatic trap. The trap is composed by the magnetic field and by a potential well between the injection and extraction side. When used as a charge breeder, 1+ ions are injected through the extraction by lowering the electrostatic potential barrier for a short time and then increasing it again to ensure a trapping mode. Further ionizations are produced by electron bombardment. High charge states ions are finally extracted by lowering the potential barrier again. This process leads to an intrinsically pulsed beam. Typical electrons current densities are between 50 and 5000 A/cm², while magnetic field values range from 2 to 8 T, thus requiring superconducting magnets. The extracted beam is very clean from contaminants due to the very good vacuum inside the trap (no added gases are necessary to produce ionizations). Even if output charge states and efficiency are very high (e.g. ¹³²Sn³⁴⁺, with an efficiency up to 20%), from the point of view of the electrostatic confinement, the EBIS-CB has a maximum space charge capacity determined mainly by the electron beam current, its energy and the length of the trap. In order to reach a high enough capacity to accept the intensities expected for the SPES project, very high values of the latter parameters would be necessary, leading to a very expensive and complicated design. Other drawbacks of this method are the high energy spread of the outgoing beam (tens eV*q) and the limited lifetime of the electron cathode.

ECRIS sources [3] are widely used to produce high intensities beams of high charge states to feed accelerators for nuclear physics experiments. In such sources the plasma is created by a resonant interaction between an electromagnetic wave fed into the source and free electrons and

it is confined by a particular magnetic configuration, called B-minimum structure. This configuration is created by superimposing an axial field generated by two or three coils for axial confinement and a multipolar field (usually a hexapole) for radial confinement. When used as a charge breeder, the 1+ beam is injected by modifying the injection side of the source: it is then captured, further ionized and extracted from the other side giving CW injection and extraction. First tests of an ECRIS adapted to charge breeding were done in the 90's by Prof. Geller and his group in Grenoble [4]. The process of charge breeding with ECRIS can be described as follows. The 1+ beam is injected with an energy corresponding to the high voltage of the charge breeder plus a small ΔV necessary to overcome the ECRIS plasma potential (the regulation of this parameter is seen to be very important for the performances of the CB). Once the 1+ beam sees the retarding potential and the fringe field of the coils, it is decelerated and enters the plasma with a low energy (some or tens eV). The 1+ ions then interact with ECR plasma ions through elastic collisions [5] leading to thermal equilibrium; they also undergo ionizing collisions, increasing their charge states. The ions lost by the magnetic trap are then extracted as a high charge states beam. Qualities of this CB are robustness and reliability, great intensity acceptance, possibility to have CW or pulsed beams and absence of limitation due to the quality of the injected beam. Drawbacks are the lower output charge states compared to EBIS-CB, the difficulty of breeding light elements and the presence of a stable background of contaminants as seen in the spectra acquired at the output. Anyway, this last issue can be limited by paying attention to the cleanliness of all the parts exposed to vacuum. Also, the efficiency was always lower than the EBIS-CB except for recent results obtained at Argonne National Laboratories [6].

8.2.3 The SPES Charge Breeder

As a consequence of the above explained points, an ECRIS type CB was chosen for the SPES project. The main point is that it is the only device that will be able to accept the high intensity radioactive beams expected for the SPES CB; another reason is the long time experience on ECR sources at LNL.

In particular, the SPES-CB will be developed on the basis of the Phoenix booster in operation at LPSC (Grenoble) [7-8]. This device was developed since the 90's and, in the following years, demonstrated its ability to charge breed radioactive ions, as shown in [9]. It is now in operation at TRIUMF [10]. A picture of the injection side and part of the Grenoble CB is shown in figure 8.2.

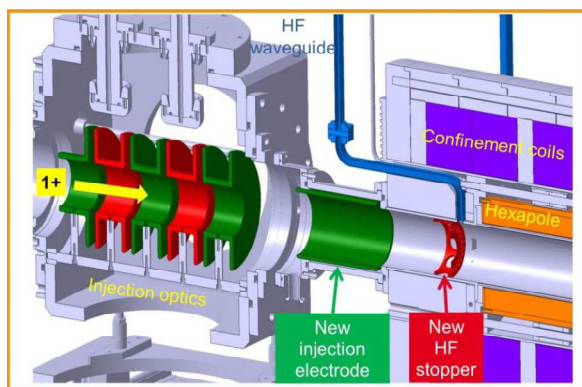


Figure 8.2: injections side and part of the Phoenix Charge Breeder developed at LPSC Grenoble (kindly furnished by Thierry Lamy).

The performances of the Phoenix CB perfectly fit with the requirements of the SPES project: the A/q ratio of the extracted charge bred ions is peaked around 6 and its emittance is

largely lower than the acceptance of the following accelerators complex (recent measurements gave $4 \cdot \epsilon_{\text{rms}} \approx 60 \pi \cdot \text{mm} \cdot \text{mrad}$). Recent results [8] showed an increase in performances that led to values of efficiency close to the ones obtained with the EBIS-CB with gases, as shown in the following table.

Table 8.1: recent performances of the Phoenix CB [8]

Element	Charge State	Efficiency [%]	CB time [ms]
Ar	8+	16.2	78
Xe	20+	10.9	252
Rb	17+	7.5	226

By summing over all the charge states of charge bred ions, a global capture of almost 80% was found for Ar and Xe, while 50% was obtained for Rubidium (tutte sigle o tutte parole). This difference is mainly due to the fact that, when a 1+ gaseous ion is lost on the chamber wall, it can be recycled and captured again by the ECR plasma; this doesn't happen in case of condensable elements due to walls sticking, leading to a lower global capture. The improvement of the capture efficiency even for condensable elements is under study by INFN in the framework of the EMILIE project [11].

The CB beam line has been designed in order to have the possibility to characterize the source in advance, before injecting radioactive ions into it. For this reason, a system for production, focusing and selection of stable 1+ beams will be implemented. A schematic drawing of the entire beam line is shown in figure 8.3. The 1+ source will be an adaptation of the ones already in use for the Target-Ion Source system i.e. a surface ionization source for the production of alkali metals like Rb and Cs and a plasma source for the production of beams from gaseous elements. The extracted 1+ beam will be focused by means of an electrostatic lens and the desired beam will be selected by a 90°, 0.5 m radius bending dipole. The resolving power of such a dipole will be $\sim 1/150$, with appropriate selection slit.

The selected 1+ beam will be characterized in terms of current and beam quality and then injected into the CB through an electrostatic triplet. The possibility of using a grounded tube to inject the 1+ beam has been foreseen, although the real need of such a system will be clarified by experiments that will be performed in 2013 at LPSC and ANL. Once the 1+ beam will be charge bred and extracted as an n+ beam, it will be focused by an electrostatic triplet forming a waist before injection into the n+ downstream spectrometer (MRMS – Medium Resolution Mass Spectrometer). This will help to increase the resolving power of the spectrometer and will also allow to measure the beam current extracted by the CB in order to check the transmission through the beam line.

Special attention has been paid to the design of the MRMS: in fact, as written above, the ECRIS-CB has a non negligible background that can cause overlapping of undesired ions with the charge bred radioactive ones. After considering the most interesting radioactive species that will be produced (Rb, Cs, Sn, Ge) and the possible contaminants introduced by the CB (O, N, C, Ar, Kr), we opted for a spectrometer resolving power of 1/1000 at 10% of the peak's intensity. This will be accomplished by using four electrostatic quadrupoles to prepare the beam for the selection and two 80°, 0.75 m radius dipoles with skew edges. Other four electrostatic quadrupoles at the exit of the second dipole will adjust the beam at the diagnostics station, where beam current and emittance will be measured. The n+ beam will then be delivered to be post-accelerated. Further details on the MRMS can be found in section 8.3.2.

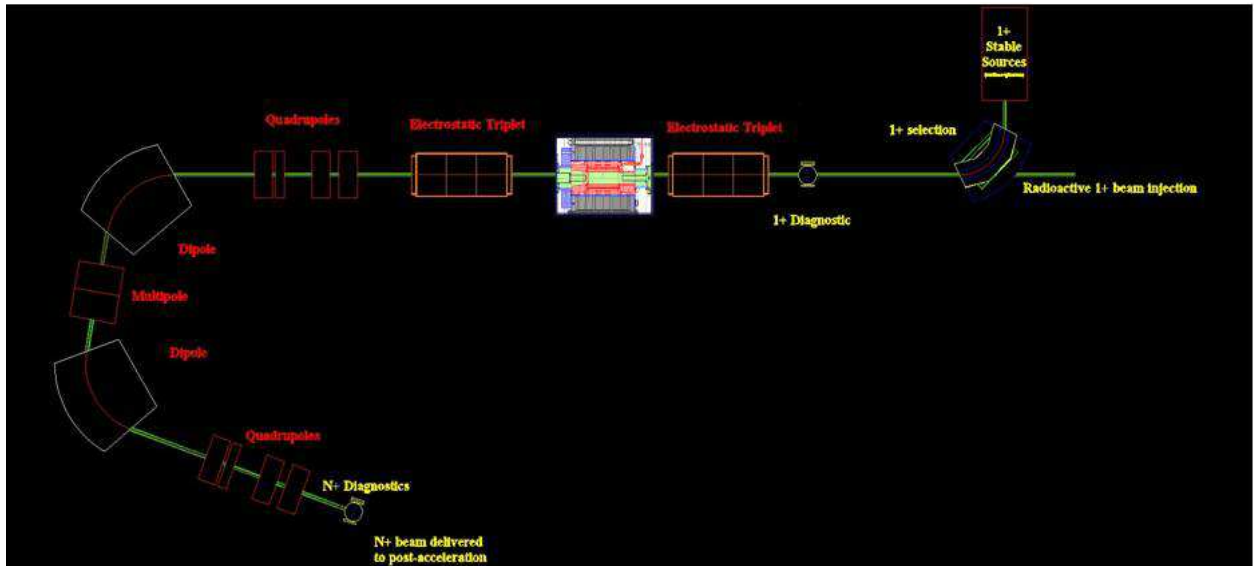


Figure 8.3: Schematic drawing of the CB beam line for the SPES project.

8.3 The SPES RNB Injector and Refurbishment of ALPI Lattice

8.3.1 Introduction

In the SPES project framework, a new injection line will be built to transport and match the RNB from the CB to the existing ALPI superconducting linac. This chapter describes the injection line from the CB to ALPI (including a new CW normal conducting RFQ), together with the layout changes proposed for ALPI itself, in order to make it suitable as an accelerator of up to 10 MeV/u RN beams with a high overall transmission.

It is to be noted, incidentally, that the new line shall be a third injector into ALPI, since the stable beam injection lines (Tandem and PIAVE) will remain operational. The new layout is comprehensively described in fig. 8.1.

8.3.2 Spectrometer after the Charge Breeder

A quite good spectrometer is necessary after the Charge Breeder to be able to separate ions in mass by a $\sim 1/1000$ resolution. This spectrometer is a scaled version of the HRMS, but with a higher energy of 0.76 MeV for the reference ion ($^{132}\text{Sn}^{19+}$) and a larger emittance of 0.06 mm mrad (RMS norm). The present solution is reported in the figure 8.4:

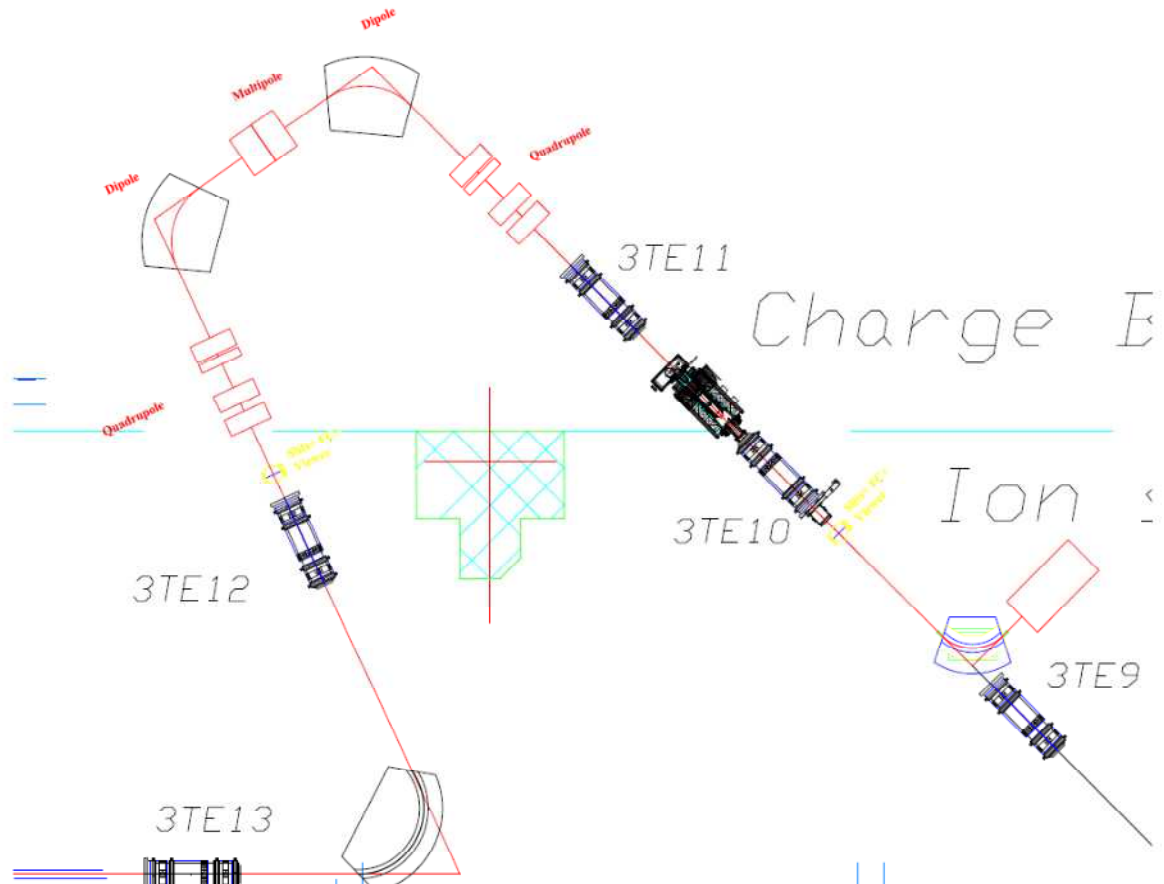


Figure 8.4: Layout of Spectrometer (MRMS) after the Charge Breeder.

The main spectrometer components are electrostatic lenses and magnetic dipoles; in addition, some electrostatic multipoles element are used in the middle and after the “U” line, so as to avoid any emittance growth (see table 8.2).

Table 8.2: Main parameters of the MRMS

Mass Resolution	1/1000
Dipole Bending Angle	80 deg
Dipole Bending radius	0.75 m
Dipole Edge	30 deg
Dipole max field	0.1 T
Energy (1/7)	0.76 MeV
Electrostatic Multipole	up to dodecapole
Electrostatic triplets max voltage	6.95 kV

The herein reported transport line is optimized for fitting the available space in the LNL 3rd experimental hall; where it is to be located; the linear dispersion of the spectrometer is 30 m and the x_{RMS} spot size is 2 mm (see the envelope in fig. 8.5).

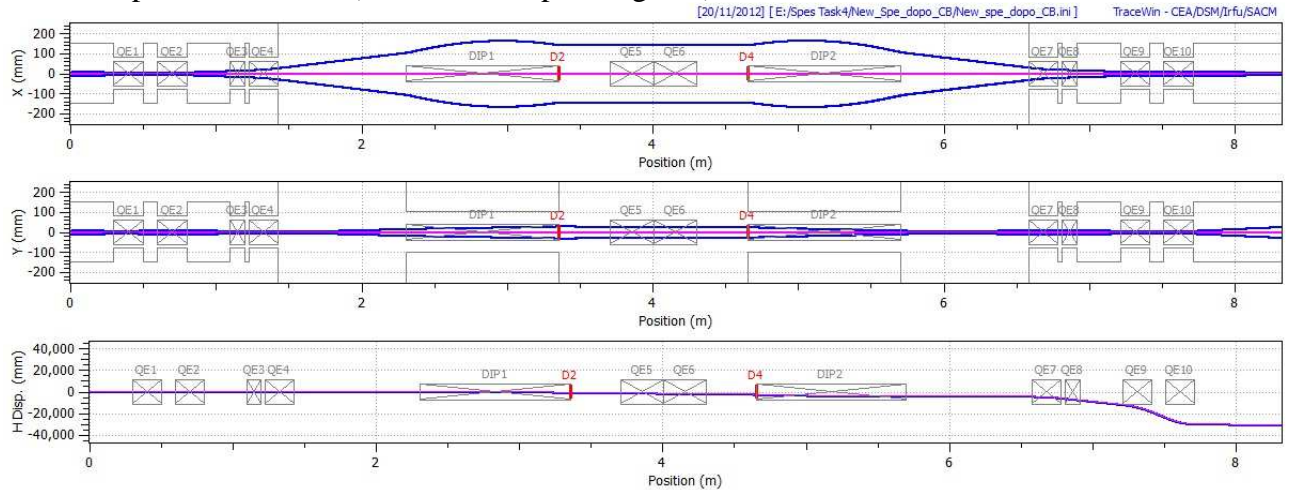


Figure 8.5: Envelope layout of the Spectrometer after the Charge Breeder.

By using the multiparticle code TraceWin [12], the resolving power can be estimated as $\sim 1/1000$ for the full size spot, as reported in following figure 8.6:

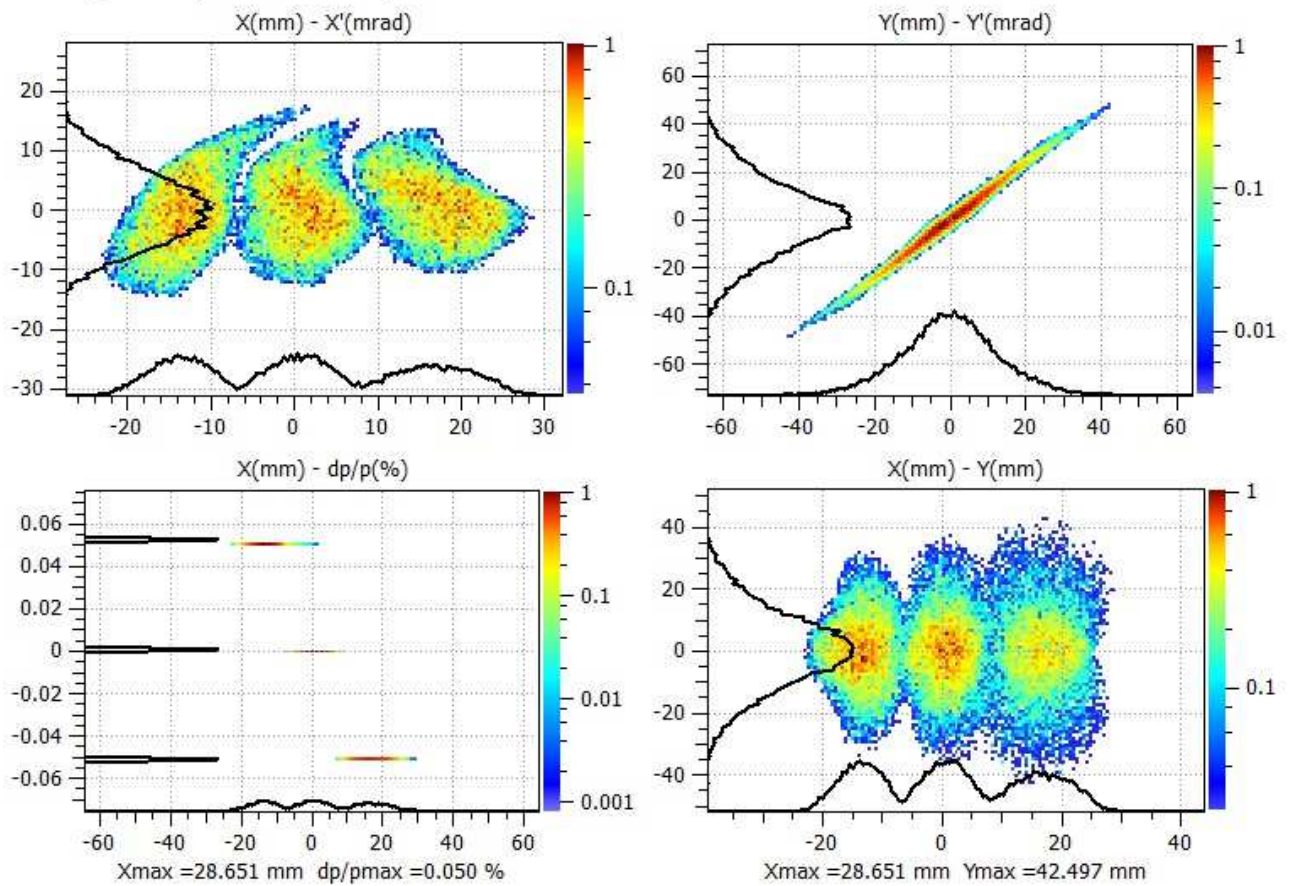


Figure 8.6: MRMS spectrometer resolution.

In the same figure, it is assumed that the nearest contaminant beam has the same emittance and intensity as the nominal one.

8.3.3 Transport Line to the SPES RFQ

The transport line is made of electrostatic triplets, as in the line from the HRMS to the CB. The main parameters are reported in table 8.3. In figure 8.7 the beam envelope in the (x,z) and (y,z) planes from the MRMS to the SPES RFQ are included: the main purpose of the line is to match the Twiss parameters at the RFQ input, without any beam loss. A careful vacuum level (10^{-8} torr) is required in this beam line to avoid charge exchange due to scattering induced losses [13]. Figs. 8.8 and 8.9 report the evolution of normalized emittance on this beam line, and the phase space at the output of the RFQ. The distance from the last electrostatic triplet and the RFQ input is 300 mm.

Table 8.3: Main parameters of the transport line to the SPES RFQ

Ion		132Sn19+
Electrostatic lengths (mm)	Triplet	170+40+480+40+170
Electrostatic radius	Triplet	60 mm
Electrostatic max voltage		4.1 kV
115° Dipole Radius		750 mm
115° Dipole max field		0.1 T
115° Dipole Edge		38°
Total number of triplets		8

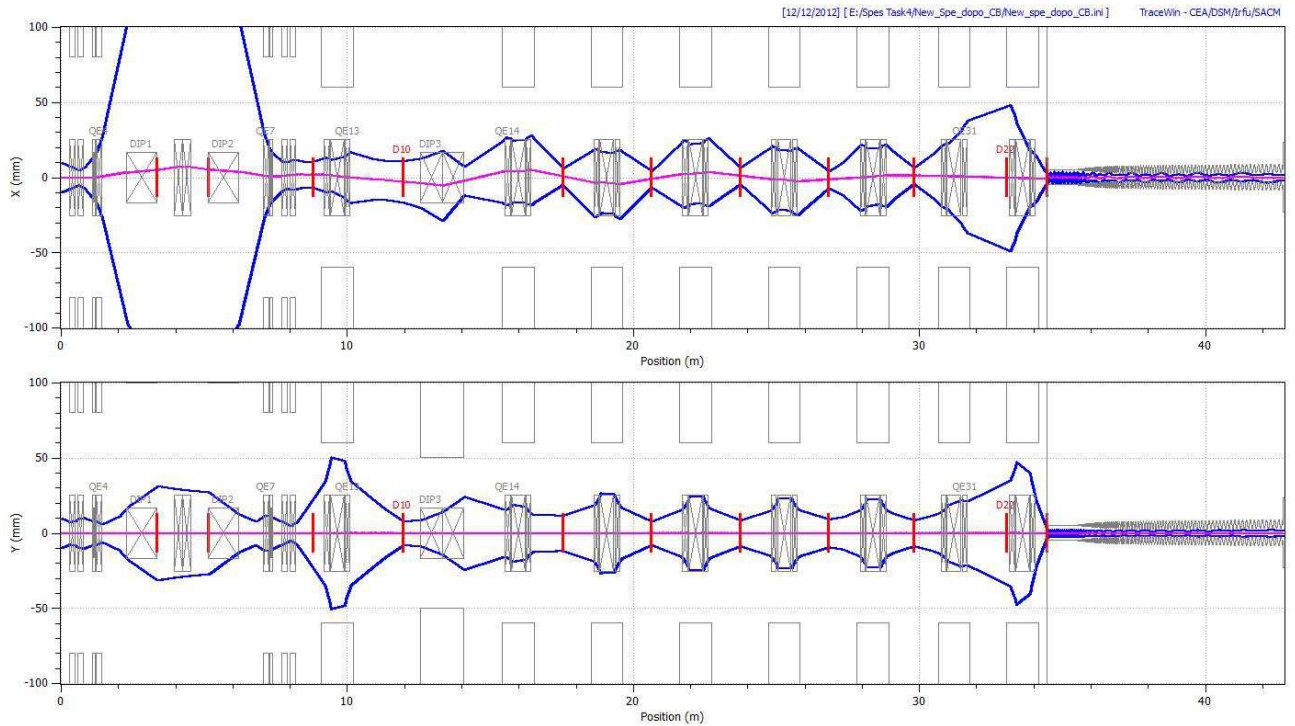


Figure 8.7: Multiparticle beam layout from the CB to the end of SPES RFQ.

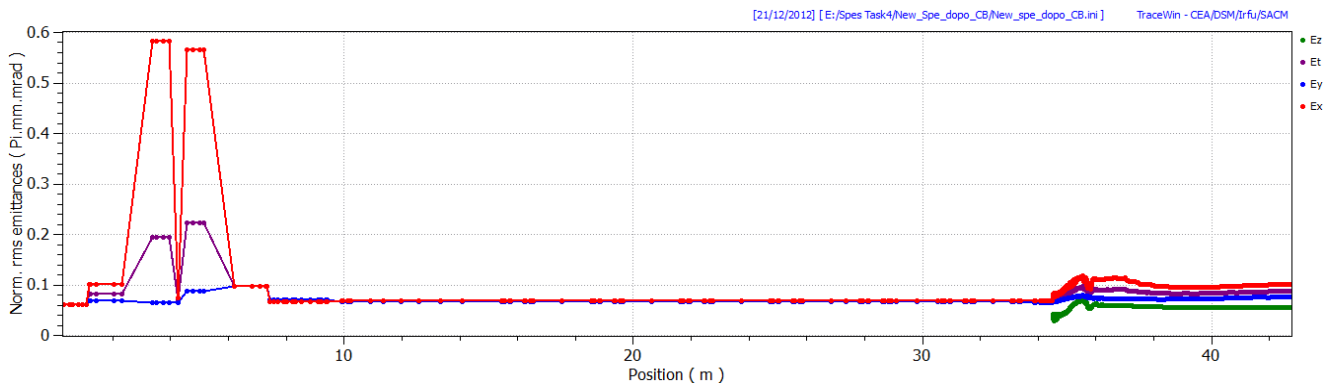


Figure 8.8: Emittance evolution from the CB to the end of SPES RFQ.

Ele: 489 [42.743 m] NGOOD : 84553 / 84553

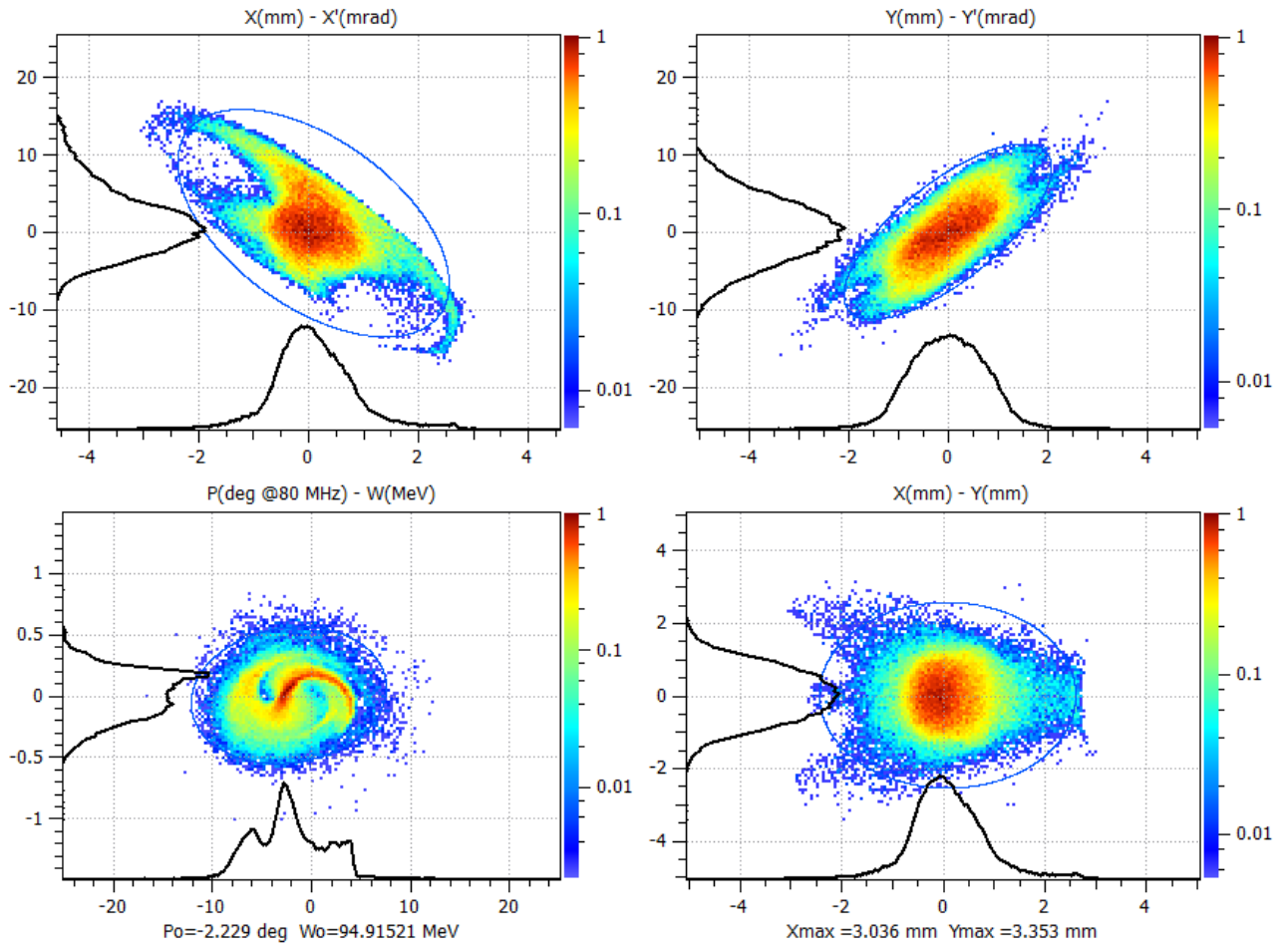


Figure 8.9: Phase Space at RFQ output.

8.3.4 The SPES RFQ

This SPES injector into ALPI includes a new RFQ (see Tab. 8.4) that will operate in a CW mode (100% duty factor) at a resonant frequency of 80 MHz. This frequency is the same as that of the superconducting structures of lowest energy in ALPI. The ion injection energy was set to 5.7 keV/u. This choice is a compromise between the desire of reducing the ion energy to simplify the LEBT and the RFQ bunching section design and the need to increase the injection energy, so as to increase the beam rigidity in the spectrometer and to reduce space charge effects. The extraction energy was set to 727 keV/u (with respect to the 588 keV/u of the existing SRFQ of the stable beam PIAVE injector), to optimize the beam dynamics of the superconducting linac ALPI.

Table 8.4: Principal RFQ parameters

Parameter (units)	Value
Operational mode	CW
Frequency (MHz)	80.
Injection Energy (keV/u)	5.7 ($\beta=0.0035$)
Output Energy (keV/u)	727 ($\beta=0.0395$)
Accelerated beam current (μA)	100
Charge states of accelerated ions (Q/A)	7 – 3
Internal bunching section	Yes

The design goals were to minimize the longitudinal and transverse emittances growth and to optimize the RF losses and beam transmission of the RFQ structure. The RFQ cells were created using the program CORTO [14](also adopted for the design of CERN Linac3 RFQ), the PARMTEQ code package [15] and Toutatis [16], in an iterative cell-by-cell procedure. With this design the RF power consumption is minimized. A transition cell was used at both the entrance and exit of the RFQ. At the exit side, a radial matching section with an appropriate length after the transition cell was also used so that the output beam has the same Twiss parameters in both the horizontal and vertical planes. Table 8.5 and Figure 8.10 show the main parameters of the RFQ. The RFQ transmission is more than 95% of accelerated particles, and the final longitudinal RMS emittance is 0.15 nskeV/u. The 99% longitudinal emittance is 1.2 ns keV/u (see figures 8.10 and 8.11).

Table 8.5: RFQ design parameters

Parameter (units)	Design 1
Inter-vane voltage V (kV, A/q=7)	63.8
Vane length L (m)	8.27
Average radius R_0 (mm)	5.03 – 5.769
Vane radius ρ to average radius ratio	0.8
Modulation factor m	1.0 – 3.03
Total number of cells	343
Synchronous phase (deg.)	-90 – -20
Focusing strength B	5.28 – 4.06
Peak field (Kilpatrick units)	1.7

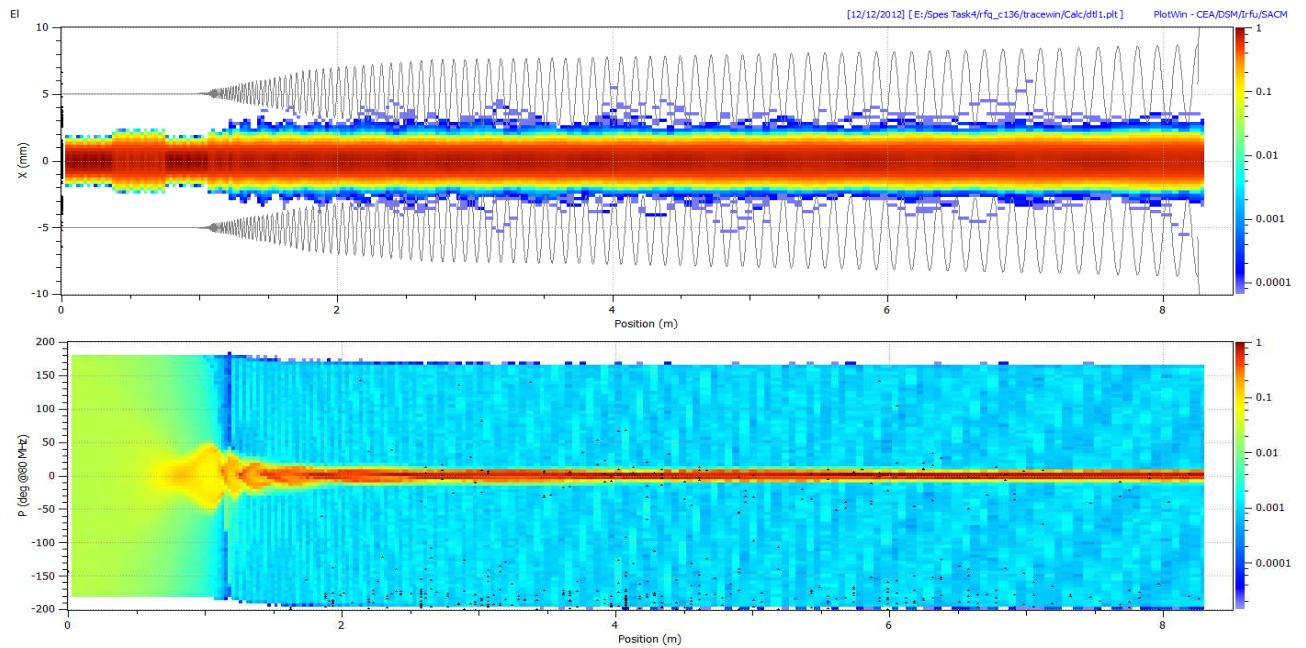


Figure 8.10: X envelope and phase density along the RFQ.

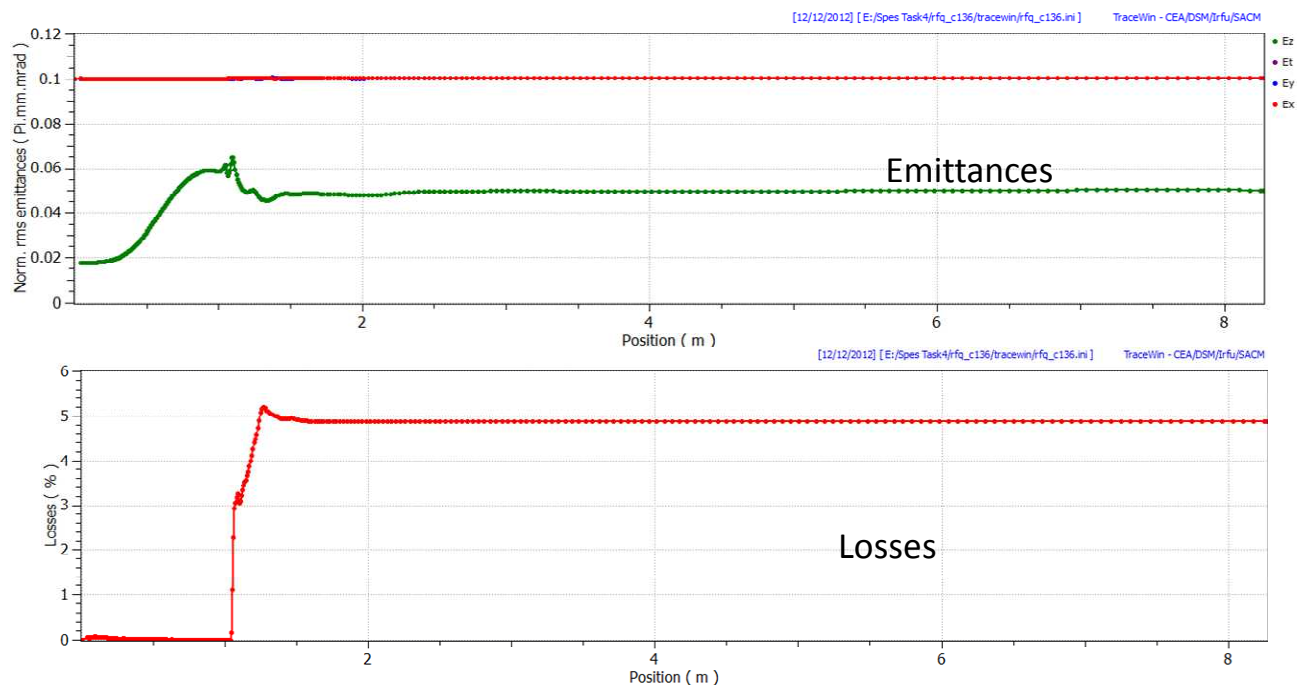


Figure 8.11: RMS emittance and losses along the RFQ.

The SPES RFQ will be normal conducting and operating in the CW mode, its size being similar to the one which is being built for the SPIRAL2 project [17].

We propose a four vane structure, divided in 8 modules of approximately equal length. The cylindrical tank (800 mm diameter) is in Cu-plated iron, properly annealed. The electrodes are built out of OFE copper and 316LN stainless steel; brazing under vacuum will be used to build the cooling channels and the interface reference surfaces between electrode and tank.

The electrode modulation will be milled to the final value after brazing, and as the last operation the electrodes are positioned, aligned and bolted to their final positions in the tank. Vacuum tightness is guaranteed at electrode bases by circular gaskets, which can be inspected and substituted without removing the electrode. The RF joint is at the electrode basis, with a current limited to about 14 A/cm even in the undercut region (see later).

In Figure 8.12 the cross sections of the cavity corresponding to the Low Energy and High Energy RFQ Sides are shown. It is possible to notice that the minimum value of W_b is about 2.3 cm and its maximum value is 3.0 cm. It should be noticed also that the maximum current density at the RF joint is 12.6 A/cm.

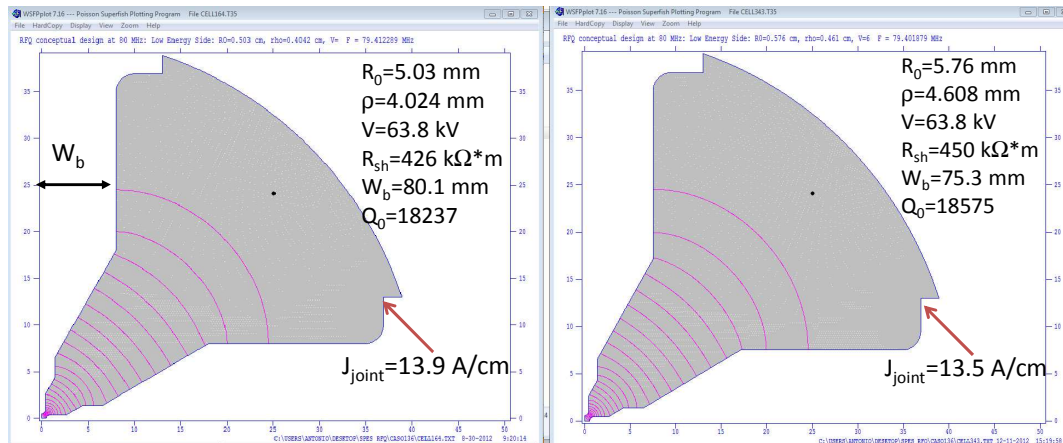


Figure 8.12: The Low Energy (left) and High Energy (right) cross sections of the RFQ.

As to power consumption calculations, it has to be pointed out that the total power P_{RF} is related to the 2D power calculated by SUPERFISH, by means of the relationship

$$P_{RF} = P_{SF} \alpha_{3D} \alpha_{RF}$$

where $\alpha_{3D}=1.3$ is a factor that takes into account the 3D losses, $\alpha_{RF} = 1.2$ takes into account the margins for the RF System losses (losses in the lines and in the circulator, finite bandwidth of the amplifier etc). In the following table the main RF parameters are shown.

Table 8.6: Main RF parameters

Shunt Impedance (SF)	426-450	k Ω ·m
Q0 (SF)	18000	
Copper power (SF)	80	kW
Stored Energy	2.9	J
Max H field (2D)	1400	A/m
Max Power Density (2D)	0.25	W/cm ²
Total Power	125	kW

The RF power will be fed by a single amplifier unit based on a TH535 tube (180 kW max power in CW).

The vane terminations and undercuts are the regions of maximum power density, and have to be properly cooled. Moreover, with bolted electrodes one has to be careful about the

maximum current across the RF joint at the basis of the electrodes. The design proposed (Fig. 8.12) is such to keep the current density always below the value of the 2D cross section.

HFSS [18] simulations showed that, at the electrode base where the RF joint is foreseen, the maximum current does not exceed 14 A/cm (evaluated from Superfish, and shown as a dashed line in fig. 8.13).

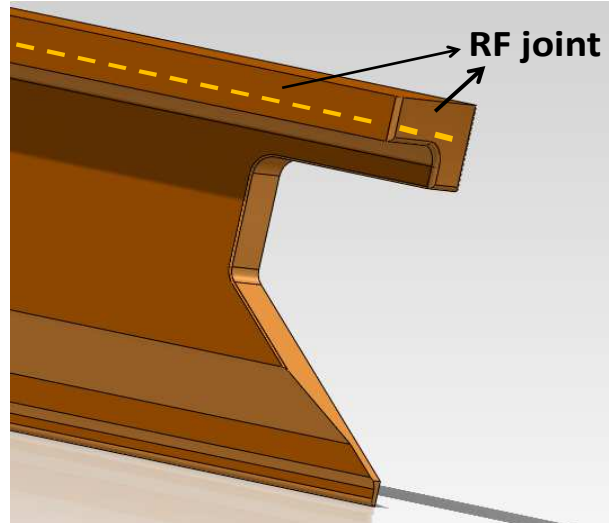


Figure 8.13: Detail of the electrode on the High Energy Side of the RFQ, with the location of the RF joint.

Some comments have to be made on the tuning range of the structure, related to the construction and alignment tolerances. The sensitivity with respect to geometrical errors was numerically addressed, and it was found that the sensitivity is $\chi_{R0} = \partial f / \partial R0 = 3.6$ MHz/mm. This means that a 0.2 mm misalignment of one electrode gives a frequency shift of $720/4$ kHz = 180 kHz. Therefore, in order to allow positioning the electrodes with ± 0.2 mm precision, a tuning range of ± 720 kHz is needed. It has also to be pointed out that, due to the favourable L/λ ratio of this RFQ, the 1st upper quadrupole mode is about 2.1 MHz away from the fundamental one. As a consequence, the tuning range can be used mainly for compensation of misalignments. To tune the structure, a system of slug tuners has to be foreseen. The high value of the shunt impedance*length for such a structure and the power capability of the RF source allow the implementation of a rather large tuning range.

8.3.5 Beam Dynamics of the Matching Line between RFQ and ALPI

The matching line between the SPES RFQ and ALPI, has the task to perform a quite long beam transport (~ 20 m), without introducing any degradation; the beam in the longitudinal plane is kept focused by means of 3 normal conducting bunchers, similar to HEB1 and HEB2 of PIAVE, with a maximum strength (E_0TL) of 111 kV, for the reference ion $^{132}\text{Sn}^{19+}$ ($A/q=7$), in the buncher located nearest to the SPES RFQ. In figure 8.14 the envelope lines from the SPES RFQ to the low beta cryostats of ALPI are reported.

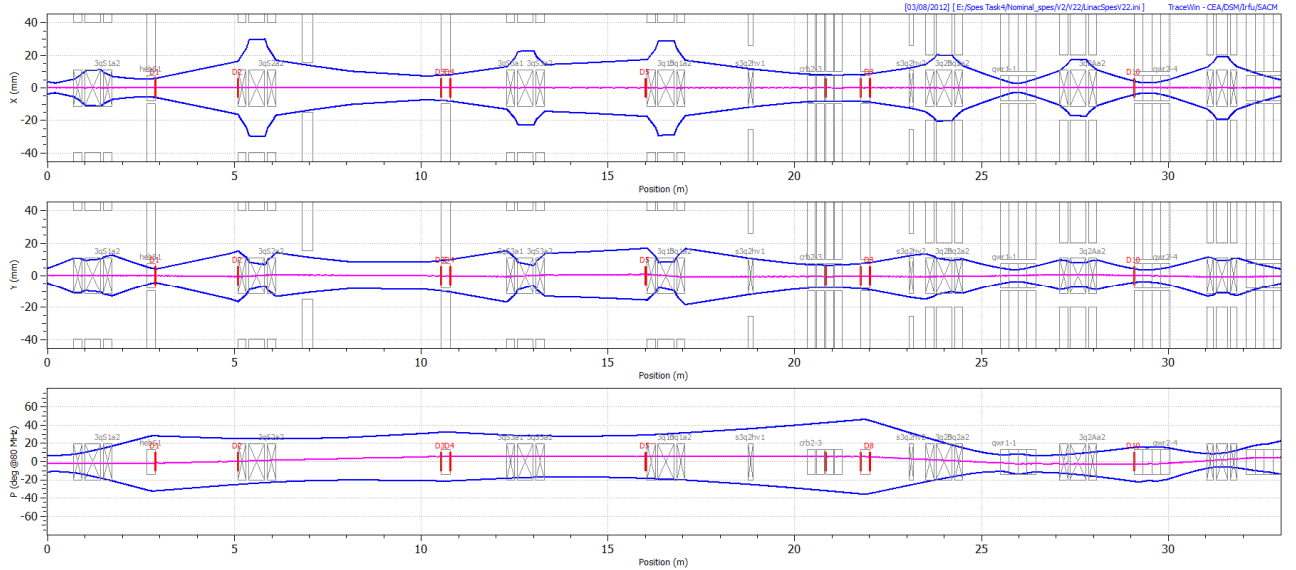


Figure 8.14: Multiparticle beam envelopes from the new RFQ to CR03, from left to right.

8.3.6 New layout of the superconducting linac ALPI in the SPES framework

The present configuration of the LNL super-conducting accelerator linac (ALPI) fits the requirements for SPES post acceleration too. Nevertheless, an upgrade of its performances both in overall transmission and final energy is needed, such upgrade is obtained by elaborating a layout which minimizes the impact on the present one [19].

The super-conducting linac ALPI is injected, at present, either by the XTU tandem or by the SC PIAVE injector (see Fig. 8.1). The linac (at the present 68 accelerating cavities for a total equivalent voltage of 48 MV) consists in two branches connected by an achromatic and isochronous U-bend: these are referred, in the following, as low-energy and high-energy branches. The ALPI period consists in one triplet and 2 cryostats (4 cavities in each cryostat), and a diagnostic box (profile monitor and Faraday cup) in between.

The PIAVE-ALPI complex is able to accelerate beams up to $A/q \sim 7$. Higher A/q ions suffer from too low injection energy into the medium- β cryostats, where the RF defocusing is too strong and the beam gets easily lost onto the cavity beam ports. In the latest years the average cavity accelerating field in ALPI has been enhanced by more than a factor of two with respect to the original design value. The strength of the focusing lenses, on the other hand, has remained the same, i.e. 20 T/m; therefore, even for $6 < A/q < 7$, it is hard to design a proper longitudinal beam dynamics without beam losses in the transverse phase space. To fully exploit the available acceleration gradient, some improvements are required in ALPI layout. The just accomplished upgrade of ALPI cryogenic plant has provided an increase in the refrigeration power by more than 300 W (from 700 to more than 1000 W), thus providing adequate redundancy and leaving ~ 100 W available for new cryogenic installations.

In this framework, it has been proposed to promote the presently “bunching” cryostats CRB2 and CRB4 (at the beginning and end of ALPI) to the role of “accelerating” cryostats CR21 and CR22, equipping them with 8 additional Nb-sputtered QWRs.

The role of the 160 MHz buncher CRB2 can be taken by the already existing 80 MHz NC buncher HEB2 in case of relatively light beams injected by the Tandem into the 160 MHz medium β_{opt} section directly, without significantly increasing the beam loss (this will be verified experimentally in 2013).

Two QWR cryostats, available at present in the PIAVE injector, shall be relocated in positions CR01 and CR02 (presently empty) in order to accelerate the SPES Radioactive Ion Beam (727 keV/A) to a sufficient beta for injection into the present ALPI configuration.

The layout of the new very-first section foresees a different period: CR01, triplet, CR02, triplet, so as to reduce the longitudinal phase advance (see the envelopes in figure 8.15). The remaining layout of the linac will remain unchanged.

In this scenario, the average operational values of the accelerating fields will be: CR01 and CR02 at 4 MV/m, CR03-CR18 at 4.5 MV/m and CR19-CR22 at 6.5 MV/m. These values are consistent with well-proven on-line experimental results.

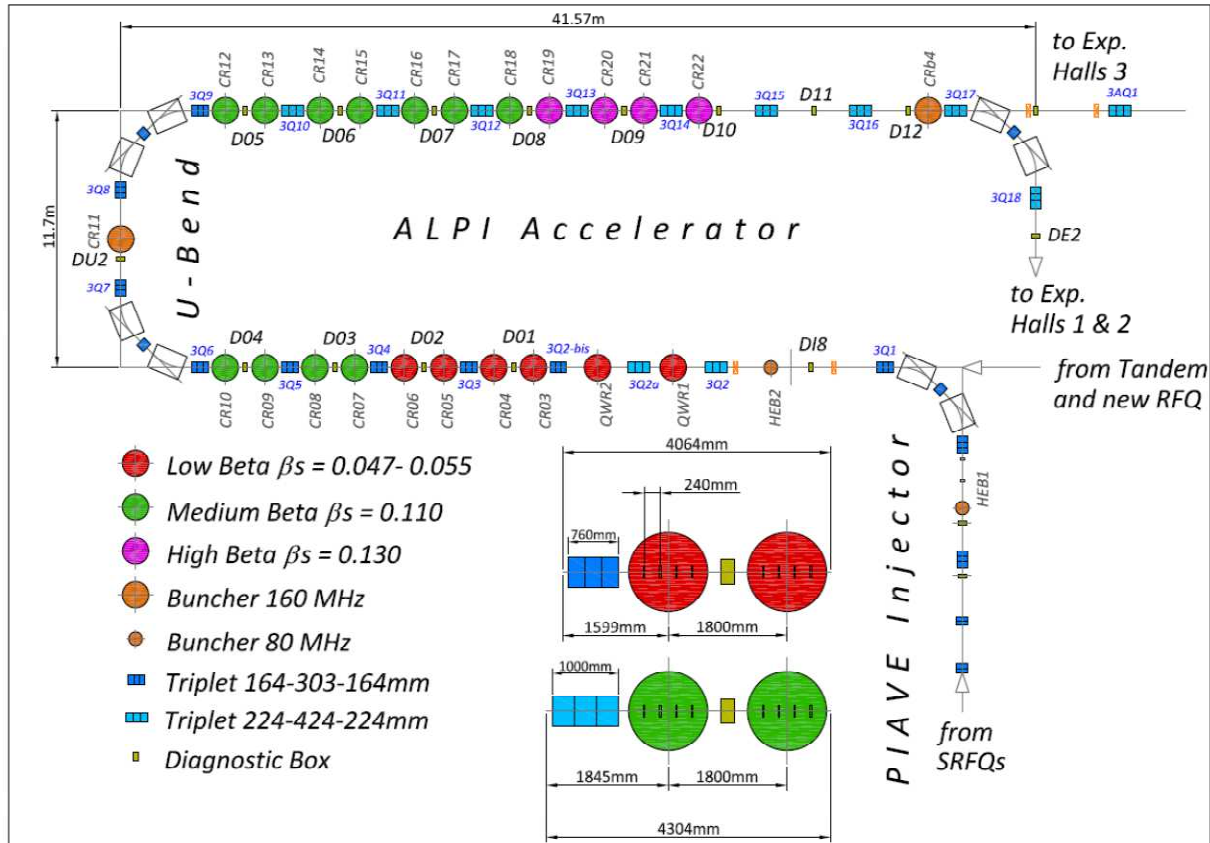


Figure 8.15: New ALPI Layout: the low beta (red circles), begins with a shorter period.

By using this new ALPI layout and thanks to the features of the new RFQ injector (fig. 8.16), the losses in the ALPI linac are reduced to ~ 6%: 3% in the low-E branch of the linac and the other 3% in the high-E branch of the ALPI linac (see figure 8.17). The input distribution is assumed to be gaussian at 3σ , with a longitudinal phase cut at $\pm 50^\circ$. In the design of the new injector, we assume having a beam emittance twice larger than the ones measured on PIAVE beam, in order to be on the safe side.

The beam is focused in between cryostats with a spot size of about 0.3 mm RMS. In the first half of ALPI the synchronous phase is set to $\pm 20^\circ$ (as needed to focalize/steerer the beam and to reduce the longitudinal phase advance). After the U bend of ALPI, the cavities phase is set to -20° .

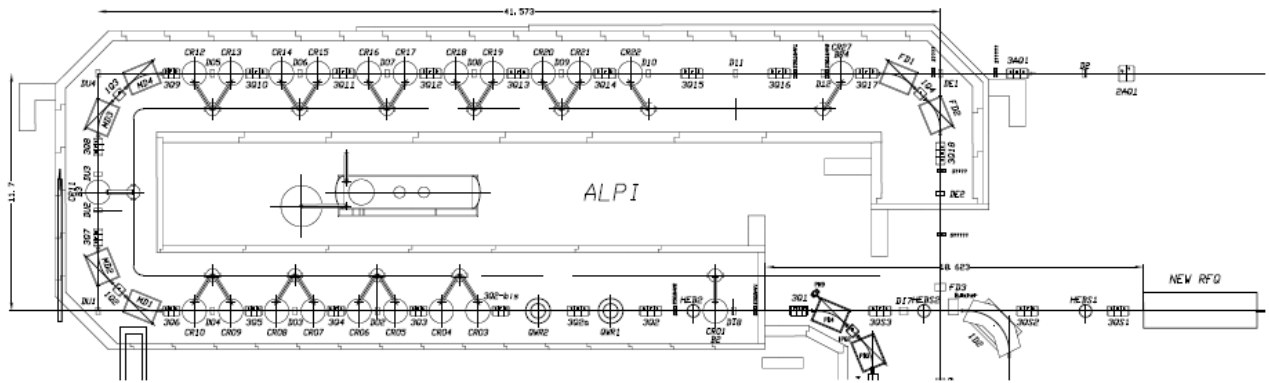


Figure 8.16: Layout of ALPI with the new RFQ as Injector.

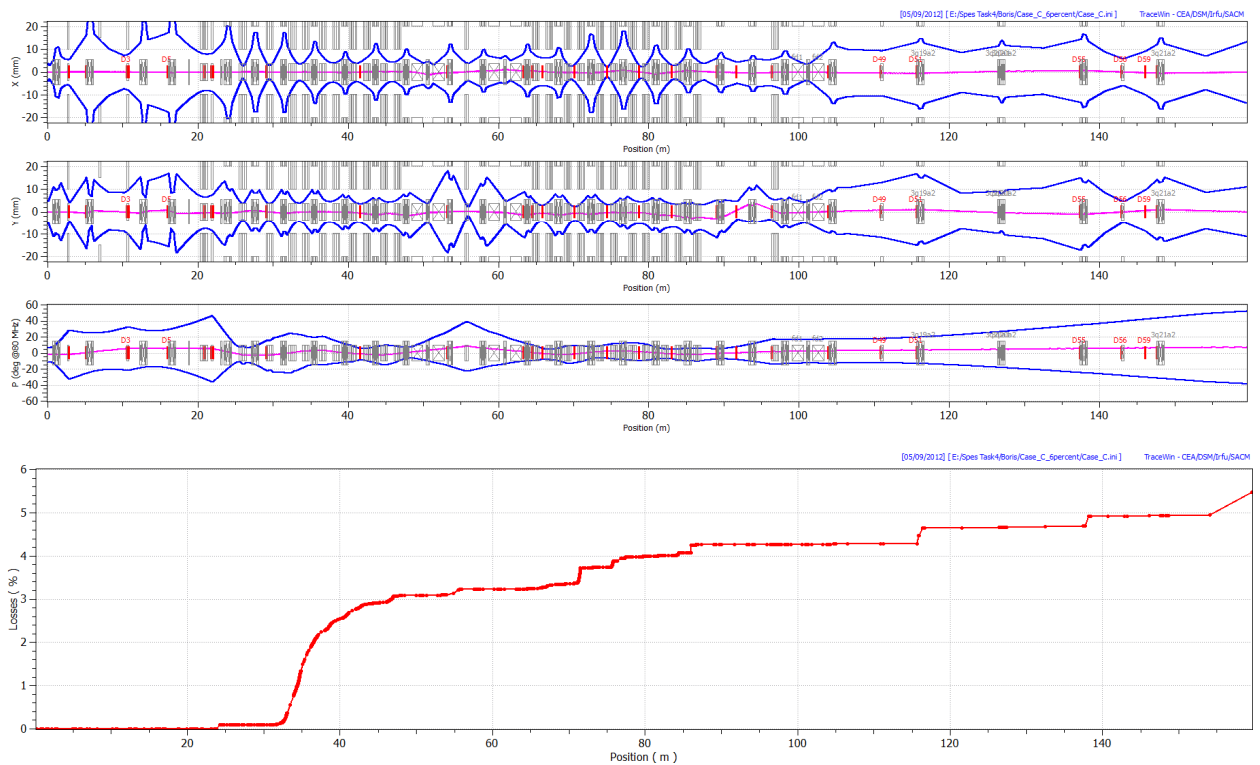


Figure 8.17: Multiparticles beam envelopes of the ALPI and losses, with the beam coming out from the new RFQ, from left to right.

Table 8.7: PIAVE-ALPI versus new RFQ-ALPI

Parameter [units]	PIAVE-ALPI	new RFQ-ALPI
A/q	7.0	7.0
Output Energy [MeV/u]	10.1	10.3
Output RMS Long. emittance [degkeV/u]	18	32
Alpi Transmission [%]	88	94
Total Transmission [%]	62	90

In table 8.7 a performance comparison between PIAVE and SPES RFQs, as injectors of ALPI, is reported. The new RFQ shows a better global transmission, mostly due to its efficient internal bunching section.

The low longitudinal emittance, produced by the new RFQ, plays an important role allowing a good transport through ALPI. On the other hand, at the linac end, this high transmission can induce a larger beam emittance on the longitudinal plane.

An upgrade of ALPI triplets has been taken into account in order to increase the machine performances. In this scenario these triplets are the principal limit, i.e. their maximum quadruple gradient 20 T/m does not permit to reduce the losses to zero with any injectors. The actual limit on output energy is also connected to the dipole maximum rigidity at the end of ALPI and to the problems/costs connected with the installation of new cryostats.

The following paragraphs will cover the major improvements, required to make ALPI an appropriate and refurbished accelerator for a reasonably long period of time. Specific upgrade measures regard both the low-beta section, with an improvement of the operational accelerating fields (par. 8.4), and the addition of more cryostats with accelerating cavities in the high beta section at the end of ALPI, to exceed $E_f=10$ MeV/A for radioactive nuclear beams (par. 8.5). Moreover new diagnostics station is foreseen in order to be suitable for both stable (and pilot) and RN beams (par. 8.6). Rejuvenation measures can be considered those on the cryogenic plant (par.8.8), to be implemented in addition to the increase of the cryogenic power capability which has been recently achieved. Preliminary considerations about replacement of vacuum and forevacuum pumps, together with the possible requirement of common storage of pump exhaust due to radioprotection requirements are being made too (par 8.7).

8.4 Upgrade of ALPI “Low Beta” Section

8.4.1 Introduction

Several upgrades are necessary for ALPI, in order to serve both as a RNB accelerator for SPES and as the Tandem and PIAVE booster for stable beams. Between them, the upgrade of the lower beta part of the linac was the first one to be funded.

The superconducting linac PIAVE-ALPI includes a low-beta section made of 20 bulk niobium quarter wave resonators, working at 80 MHz, with $\beta=0.047$ and 0.055 (see figure 8.18) [20].

Originally designed for operation at 3 MV/m with 7 W RF power, their high Q allows significantly higher gradient, limited at present by the existing RF system capabilities. An upgrade program has started at LNL that includes the construction of 4 additional cavities, the adoption of 1 kW RF power amplifiers and modifications of the cryostats necessary for cooling of the RF couplers. The activity program has been conducted in collaboration with TRIUMF (Vancouver, CA).

The final goal is to increase the voltage gain in the low-beta section from the present value of ~ 10 to above 20 MeV/q, allowing efficient acceleration of heavy ions with mass number around 200.

The ALPI low-beta section includes, at present, three cryostats, each containing 4 bulk niobium quarter-wave resonators (QWR's) with $\beta=0.055$ working at 80 MHz [21]. Room for one more cryostat (named CR3) was left at the beginning of the line. Two cryostats of the same type, hosting $\beta =0.047$ cavities of similar design, but with a flattened inner conductor [22], are part of the PIAVE injector, for a total of 20 low-beta cavities. These large cavities, powered by 150 W RF amplifiers, are equipped with mechanical dampers to reduce their sensitivity to ambient mechanical noise [23]. After several exposures to air followed by high pressure rinsing, during their lifetime, the resonators still have an average gradient ~ 6 MV/m with the nominal 7 W power dissipation; this gradient, however, can be maintained in operation only in exceptionally stable conditions of the He helium pressure. These low-beta QW cavities, in fact, are 100 times more sensitive to He pressure variations than Cu-based cavities ones (1 Hz/mbar vs. 0,01 Hz/mbar); in addition, they are less stiff and hence more susceptible to mechanical vibrations.

For long-term operation, to avoid cavity unlocking, the gradient is usually set within 3 MV/m in ALPI. The RF system, originally dimensioned for this gradient, allows a steady forward power of about 50 W per cavity. The resulting value of the P/E_a^2 ratio gives the minimum RF bandwidth for safe operation in ALPI, i.e. about ± 15 Hz. To increase the gradient, a higher forward power is required. Above 50 W, however, the thermal drift of the RF coupler and RF lines inside the cryostat causes excessive power losses and unnecessary dissipation of liquid helium. In PIAVE, where the cryogenic system guarantees a much more stable pressure in the helium circuit, the operation gradient can be raised up to about 4.5 MV/m.

8.4.2 Upgrade Plan

To set up the low-beta section upgrade plan, we took advantage of the experience developed at TRIUMF, where similar resonators [24] are operated above 6 MV/m by means of a more powerful RF system and cooled RF couplers [25].

The upgrade actions are the following:

1. Replacement of all the 150 W RF amplifiers with 1 kW units;
2. Replacement of all existing 80 MHz RF couplers with new ones cooled with liquid nitrogen;
3. Modification of all low-beta cryostats to allow use of the new couplers;

4. Construction and installation, in ALPI, of one additional cryostat hosting 4 $\beta=0.047$ resonators.

5. Installation in ALPI-PIAVE of a liquid nitrogen distribution system.

The upgraded cavities are expected to operate at least at 5 MV/m, giving a total voltage gain of above 20 MeV/q, as required. The average forward RF power required leaving ± 15 Hz RF bandwidth at 6 MV/m is about 200 W, but up to 600 W is required for safe long term operation and for pulsed power RF processing. In a first phase the new amplifiers were installed in the old cryostats. This allowed operation at a slightly ($\sim 20\%$) higher gradient than the previous one, since the available extra power allows operation with a narrower bandwidth. In a second phase a new cryostat, equipped with the new RF system and with the cooled couplers, was installed in ALPI, becoming the test bench for the new equipment. In a third phase, all the cryostats are modified and upgraded for coupler cooling. The work, to be performed in low-duty-cycle background in order to avoid interference with the linac operation, is still in progress though very close to completion.

8.4.3 Hardware Development

8.4.3.1 Quarter-wave resonators

The 4 new cavities are of the $\beta=0.047$ type with flattened inner conductor. Compared to the existing PIAVE ones, they have been modified in the stainless steel top flange, in order to allow removal of the mechanical damper without the need of opening the indium seal, and in the tuning plate, to allow a tuning range of about 30 kHz, three times larger than the previous one.



Figure 8.18: The low-beta cavities, in their construction phase

8.4.3.2 RF system

A 1 kW solid-state RF amplifier working at 80 MHz has been developed for us by a local company. These small size units could replace the old 150 W ones with no modification to the system. They can deliver continuously an average power up to 500 W in full reflection, and more than 1 kW in pulsed mode.

8.4.3.3 New RF coupler

The new RF coupler (fig. 8.19), inspired by the ISAC2 ones [26], has been designed in order to maintain a stable temperature with a forward power up to 500W, while limiting the thermal load to the liquid helium system within 1W. Both the inner and the outer conductor are made of copper and they are thermally connected by means of a split ring piece of SHAPAL-M dielectric with high thermal conductivity. Two Teflon sliding rings reduce heat exchange with the stainless steel housing, which is shaped with a reduced section near the holding flange. The coupler is moved in and out through a rotating shaft driven by a stepping motor on the cryostat top flange with a pinion-rack mechanism on the housing. The main difference from the TRIUMF model is the 90 degrees corner near the connector, that allows keeping the overall length within 160 mm (the maximum available space in our cryostats) while leaving an effective stroke of 80 mm.

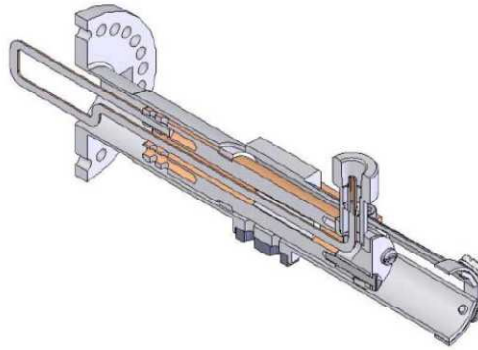


Figure 8.19: Cut view of the new cooled RF coupler

8.4.3.4 New tuning plate

The new tuning plate (fig. 8.20) for the QWRs is also a modification of the TRIUMF design. The plate is cold shaped from an annealed bulk niobium sheet with a thickness of 1.25 mm and a 264 mm diameter. A central 80 mm diameter circular flat surface is surrounded by an S-shaped deformation zone having wire-spark cut, with 24 radial slots in order both to reduce the load required for displacement and to increase the tuning range.

An aluminum cover, fixed to the plate, keeps the slots closed when the tuner is in the rest position, preventing dust contamination of the cavity during assembly. A cylindrical niobium block is welded to the centre of the flat surface, interfacing it with the mechanical tuner already in use on QWRs.

The new tuning plate allows both initial frequency adjustment at room temperature and frequency tracking at 4.2K without any further machining. The plates are capable of 14 mm displacement, going beyond yield point at room temperature, without any modification of the mechanical tuner. The corresponding frequency tuning range is about 30 kHz.

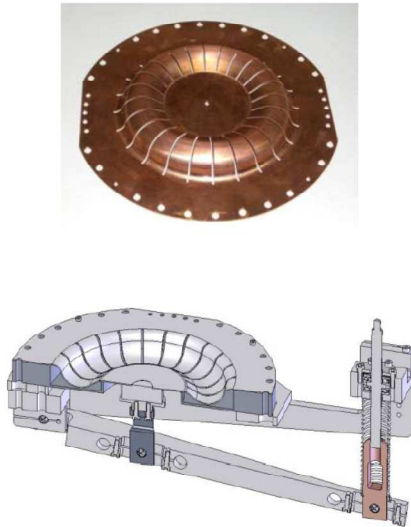


Figure 8.20: *New tuner assembly. Top: Cu prototype of the slotted tuning plate.*

8.4.3.5 Cryostat upgrade

The low-beta cryostats are being upgraded in order to cope with the increased RF power (fig. 8.21). A new line was required to bring liquid nitrogen inside the cryostat with an adjustable flow rate to fit the RF power requirements. A copper sheet, cooled to 77 K, shields the helium reservoir from the heat radiated by the RF cables. Four strips of copper braid, brazed to copper blocks linked to the liquid nitrogen pipe by tight thermal contacts, provide heat removal from the couplers. The shield, all the tubes and joints can be easily dismantled during cryostat and cavities maintenance. A serial connection of the couplers and the shield downstream ensures an efficient cooling with a LN2 flow rate of only 5 l/h.

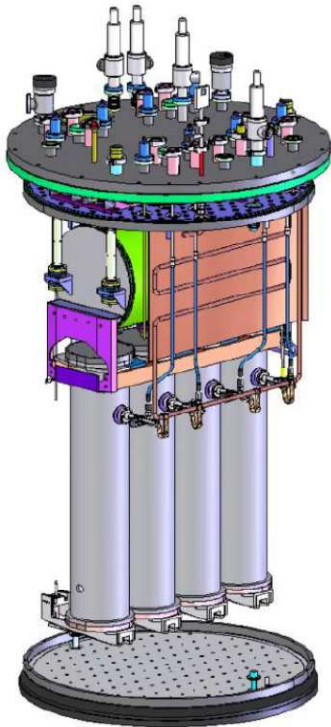


Figure 8.21. *Sketch of the modified cryostat internal part. The RF couplers are linked to a 77 K pipe via a 20 cm long strip of Cu braid. A Cu shield at 77 K prevents heat irradiation from the RF cables to the He reservoir.*

8.4.3.6 Present Status of the Upgrade Plan

Out of the four cryostats with lower beta full Nb resonators (CR03-CR06); two (CR03 and CR05) were fully upgraded and are now operational; a third cryostat is being maintained (CR04), while the intervention on CR06 is foreseen to take place within spring 2013.

Figure 8.22 shows a photo of the liquid nitrogen refrigeration system of the resonators in the CR03 cryostat. Extended tests carried out in 2010 on cryostat CR03 [5] showed that an accelerating field of 5 MV/m (at a forward power of $P_f=200$ W) could be sustained (phase-amplitude locked conditions) during 5 days. Cavities were locked even at 6 MV/m for shorter periods.



Figure 8.22: Photo of the N-cooling scheme of full Nb 80 MHz QWRs of ALPI.

It needs to be emphasized that all changes on these cryostats proceed at the low pace dictated both by the priority use of the facility to deliver beams to the experimental stations for a large fraction of the time and to the limited cryogenic crew, whose priority is on operating and fixing problems on the cryogenic plant.

8.5 ALPI Cost-effective Energy Upgrade

8.5.1 Introduction

For ALPI as an RNB accelerator, an increase in the final energy, so as to go well beyond the Coulomb barrier for nuclear reactions involving mid-A projectiles and heavy targets, is desirable.

A cost-effective E_f upgrade is proposed here: to move 2 SC buncher cryostats, which presently house a single working SC QWR but are standard cryostats which can be equipped with 4 Nb/Cu QWRs each, to the end of ALPI_(new bunchers would either be NC QWRs or a single SC cavity cryostat).

The contribution of these cryostats to E_f would be extremely effective: as an example a ^{132}Sn beam, a very attractive tool for the nuclear physics community, would reach $E_f \sim 10 \text{ MeV/A}$ with $I_{\text{beam}} \geq 1 \text{ pA}$. The upgrade of ALPI cryoplant, which increased the refrigeration capability by $\sim 30\%$, makes this change possible today.

8.5.2 Running Progress in the Final Beam Energy Achievable with ALPI

The ALPI linac has seen a continuous upgrade in the number and performance of its accelerating cavities, and consequently of the maximum achievable beam energy. An increase in beam current was, else, obtained when the required energy could be obtained using a lower more prolific charge state.

In the early nineties, the 160 MHz QWR resonators (medium β_{opt} section) originally featured a superconducting Pb layer, electrodeposited onto a bulk Cu substrate, with the rather modest average accelerating field $E_{a,\text{av}} \sim 2.7 \text{ MV/m}$ at 7W. Once the Nb sputtering technology was mature, it was successfully applied to the higher β section resonators (also at 160 MHz), the Cu substrate of which had been optimized for the sputtering deposition, achieving $E_{a,\text{av}} \sim 6 \text{ MV/m}$ and beyond. Later on, all resonators were stripped of the Pb layer and equipped with a Nb one, onto the same Cu substrates (not optimized for sputtering): the average accelerating field of the medium β section thus increased from 2.7 to 4.8 MV/m at 7W. The increase of ALPI equivalent voltage in the period 2000-2006 is shown in fig. 8.23, where the contribution of full Nb lower beta resonators (see previous paragraph) also played a role.

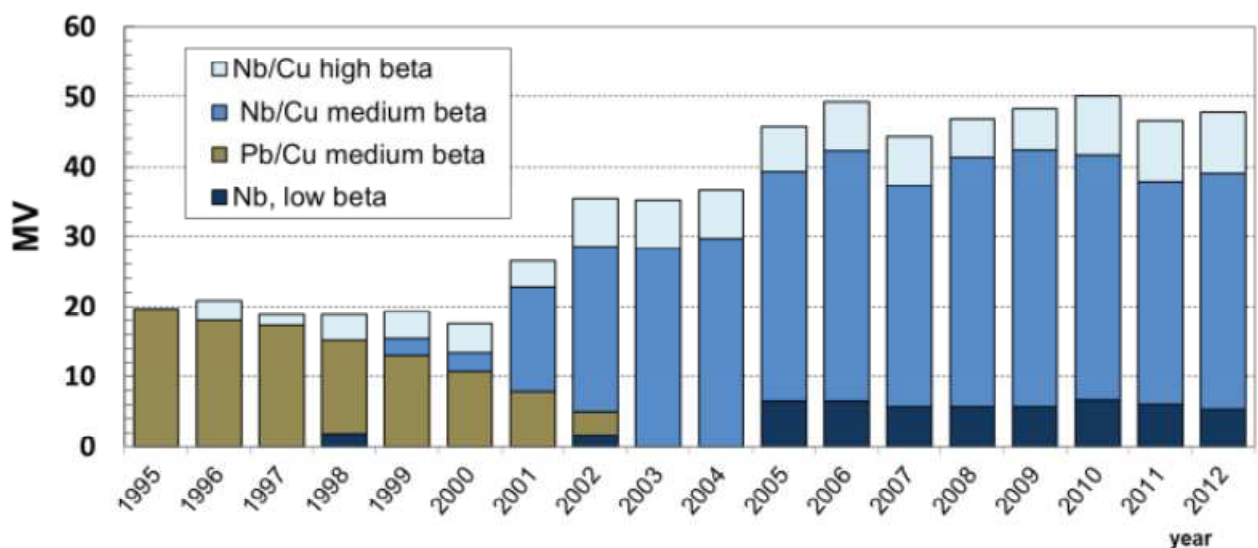


Figure 8.23: Previous upgrades of the accelerating field of ALPI resonators ended up in more than doubling the linac overall equivalent voltage.

8.5.3 Further Upgrade of the Medium Beta Resonators

As anticipated above, a further optimization of the accelerating field of the medium beta resonators can be achieved, by new substrates with geometry and construction technology suitable for the deposition of a Nb layer per sputtering [27,28].

Similarly to higher beta resonators, the design of the high-H field region in the medium β QWR resonator (connecting the central stem to the outer conductor) of a prototype ALPI cryostat (CR15) was modified, allowing for an improved quality of the SC layer there.

Differently from high beta cavities which have external beam ports screwed to the cavity, the medium β cavities need beam ports protruding into the cavity to obtain the design beta. These beam ports are no longer brazed (with a sharp corner) but rather extruded from the Cu outer conductor itself (with a rounded-off corner), as shown in figure 8.24.

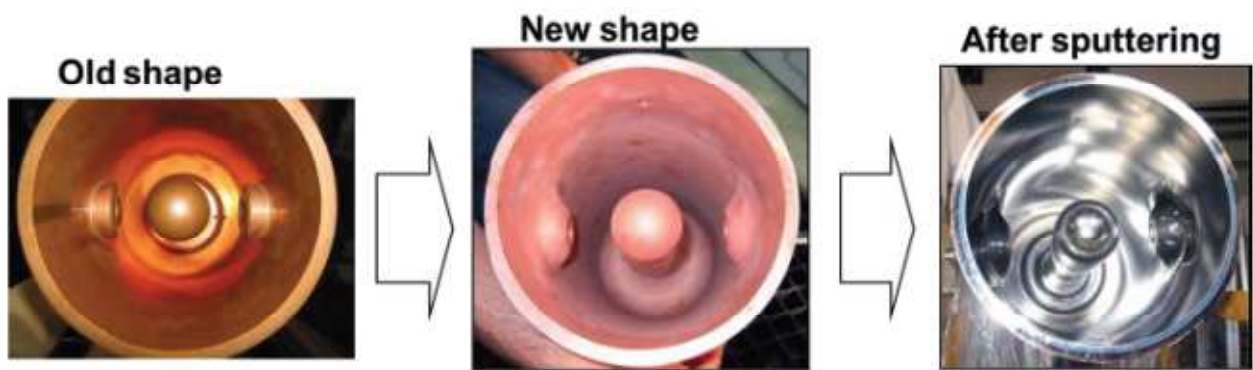


Figure 8.24: The change in shape of the interior of medium beta resonators, tested on cryostat CR15 on ALPI linac in 2012, is shown. See a detailed report in ref. 27.

As shown in [27], the results obtained on the prototype cryostat CR15 are promising ($E_{a,av} = 5.5$ MV/m at 7W), and susceptible of significant improvement, due to the long storage time that these cavities had to suffer since they were sputtered, before being assembled on ALPI.

Such upgrade, which is certainly cost-effective, is however significantly time consuming since it requires dismantling operational cryostats – one by one – while keeping all others operational for the scheduled experimental campaigns. It will be applied, in the future, for any cryostats requiring special maintenance; however, for a swifter energy upgrade of ALPI, the preferred option is different (described in the following par 8.5.5), i.e. to add 2 cryostats with accelerating cavities at the end of ALPI (positions CR21 and CR22), derived from cryostats presently housing bunching resonators.

It is to be noticed that any addition of elements at $T=4,2K$ would increase the overall cryogenic load of the linac, while the refrigeration capacity of the cryogenic plant was already absolutely marginal. For this and other reasons, the recently accomplished upgrade of ALPI refrigerator was deemed to be mandatory.

8.5.4 The Proposal for a Cost-Effective Upgrade Plan

The recent and on-going progress on the on-line performance of SC cavities made it possible to increase the final available energy of both medium-A (^{120}Sn , ^{132}Xe , ^{152}Sm) nuclei to $8.5\div 9.5$ MeV/A and heavier nuclei (^{197}Au) to 7.5 MeV/A. A further upgrade is necessary to reach 9.5 MeV/A for heavier species and more than 11 MeV/A for medium-A ones.

As anticipated above [29], a rather swift improvement in final energy can be obtained by adding two additional cryostats (CR21 and CR22) equipped with high beta resonators at the end of ALPI. The final beam energy for the reference ^{132}Sn beam would be 10.3 MeV/A with a charge state $q=18+$ (see par. 8.3).

In order to perform this task with limited expenditure, it is proposed to shift cryostats CRB2 and CRB4 to positions CR21 and CR22. CRB2 and CRB4 are identical to all other cryostats and perfectly suited to house four accelerating cavities each but, as a matter of fact, they presently house only two SC cavities each, which are used as beam bunchers. Beams injected from PIAVE (housing 80 MHz SC cavities) already by-pass CRB2 (kept off) and are re-bunched by the NC bunchers HEB1 and HEB2, the latter one being placed right after CRB2 on ALPI beam line.

Cryostat CRB2 (housing 2 160 MHz SC QWRs, only one of which is needed, and with the marginal maximum accelerating field of 0.3 MV/m), is used nowadays only with beams injected from the Tandem, when the 80 MHz section is off and the beam is sent directly into the 160 MHz medium β section (from cryostat CR07 onwards). If possible, the role of CRB2 would be simply taken in the future by HEB2: only simulations and ad-hoc experiments to be conducted during the first half of 2013 can indicate whether the smaller longitudinal acceptance of the 80 MHz HEB2 buncher is adequate to this purpose, or whether it would be a bottleneck, causing a drop in beam transmission.

In place of CRB4, at present requiring one cavity working at the maximum field of 0.36 MV/m, either two normal conducting resonators or a SC one will be needed, depending on the maximum field required.

A complete simulation of the beam transport in ALPI, with the addition of the two high β cryostats, was described in par. 8.3. The case studied is a $^{132}\text{Sn}^{18+}$ beam from the SPES injector.

8.5.5 *New Accelerating Cavities*

The 8 new accelerating cavities, to be installed in refurbished cryostats CR21 and CR22, shall be of the high- β Nb-sputtered type, as well as the new one which must be dedicated to beam bunching (CRB4).

It is proposed that the new CRB4 be a single-QWR rebunching cryostat. For homogeneity with the rest of the plant, this cryostat shall have a gaseous He thermal shield and common vacuum for thermal insulation and the beam transport.

The whole project requires modest investment, since it exploits most of the existing equipment, conveniently reshuffled: a limited readjustment of the cryogenic lines, a few additional Cu-based cavities and the addition of a single-QWR rebunching cryostat would be the higher cost components required.

8.6 Beam Diagnostics Tools for SPES Beams

This paragraph describes the R&D activity being carried out for the low-I diagnostics, required from the target-ion-source system to the final experimental stations after ALPI. After the CB, and in front of the experimental stations, two diagnostics boxes of the type described in chapter 7 (for the identification of the RA species) will be implemented too.

To control the reaccelerated beam along the RNB line, the following kinds of beam diagnostics devices are needed: beam profile monitor, current monitor, and energy and time detector.

8.6.1 Beam profile monitor

These devices should be conceived for two different beam current regimes for the following reasons. In order to drive the radioactive beam along the linac, the idea is to use first the so called “pilot beam”, a stable beam with the same RNB A/q ratio, to set up the magnet and the cavities; only once the setting with such stable beam is made, with possibly minor setup changes the radioactive beam can be accelerated. The pilot beam shall feature beam currents in the nA regime, while the RNB shall have currents of fA or less.

Due to the different range of current involved, two different diagnostics methods are needed on the same diagnostics box positions along the beam line. The philosophy adopted is to keep, up to the possible extent, the same box geometry that we have on ALPI at present and to keep also the same acquisition system. Concerning the pilot beam, the idea is to use the same grid system currently in use on the linac, with some improvements regarding the wire grid robustness and the positioning precision.

In order to monitor the position and profile of the radioactive ion beam, some new detectors must be designed, due to the very low beam current foreseen. For example, taking the various Sn isotopes as standard production from the target, the intensity goes from 5×10^8 to 1×10^5 particles per second [30], i.e. from hundreds of pA to the fA regime.

Since 2001, the LNL Diagnostics Laboratory designed and tested new detectors, such as beam position and profile monitors, based essentially on micro-channel plates (MCP) [31] as beam intensifiers. The very simple idea, for the RNB case, is to put a MCP directly on the beam line. Electrons produced on it and collected, after multiplication, on a position sensitive anode give the beam impact position [32]. A new collecting anode was used with horizontal and vertical capability on the same plane (see fig.8.25) with 0.75 mm position resolution.

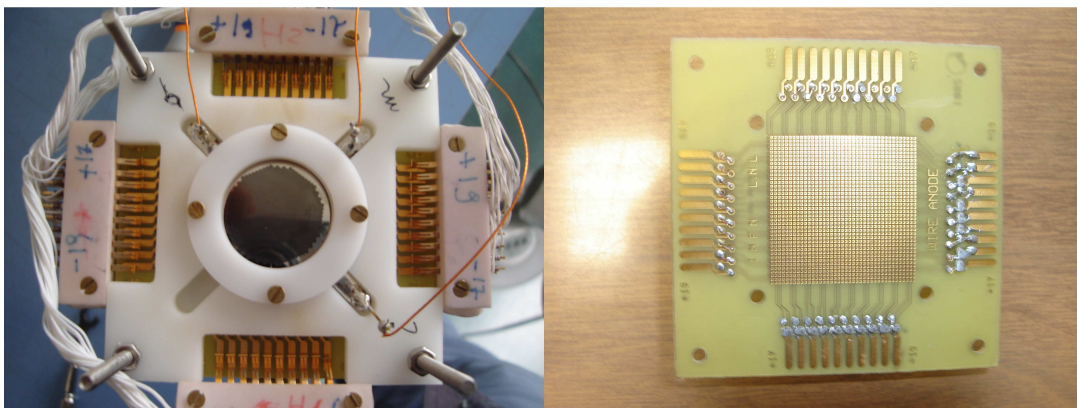


Figure 8.25: MCP system (left) in front of a collecting anode (right). The collecting anode consists of 1600 pads (40x40 in H and V direction), linked alternately to each other to form 40 horizontal and 40 vertical strips on the same plane, but not shorted together.

During the past years many tests have been performed and recently some good results have been achieved. In fig.8.26 (left) the H and V profile of an estimated 10 fA beam current of ^{40}Ca beam is shown. On the right hand side, 100 fA of the same beam is shown. The two horns on both directions are due to a screen with 2 holes, 3 mm diameter and 10 mm apart, placed in front of the MCP at 45° , so as to estimate the position resolution. In terms of particles per second, as the charge state of the beam was +9, we are in the range of 10^4 - 10^5 ions per second.

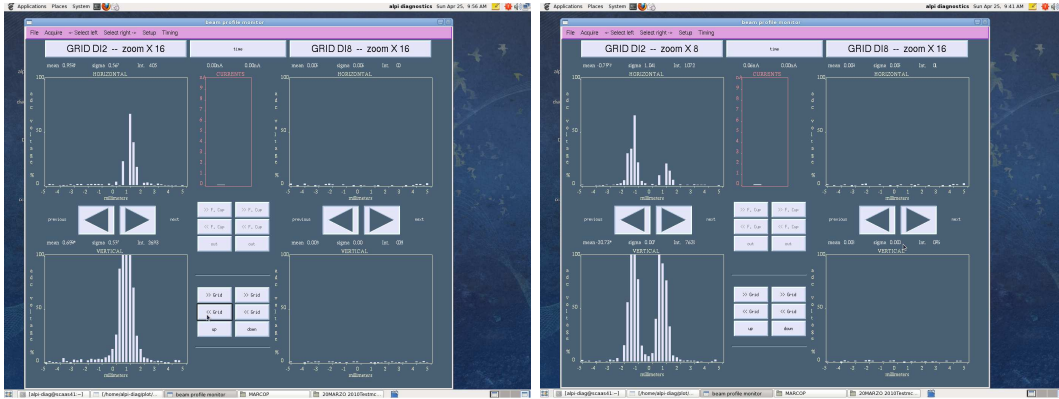


Figure 8.26: (left) beam profile (H and V) of 10 fA ^{40}Ca , (right) beam profile of 100 fA ^{40}Ca : the two horns are due to a screen with 2 holes in front of the MCP.

The front end electronics will be the same that is currently used for stable beams: hence, for the machine operator, everything will look familiar from the point of view of the diagnostic program graphical interface. Since the two detectors will be inserted into the same position within the diagnostics box, some improvements will have to be made in the management of the grid movement mechanism, to avoid mechanical interference.

8.6.2 Beam Current monitor

Faraday cup for current measurements could be an issue at the low RNB intensities. A strong R&D programme on electronics is necessary, so as to reach the signal-to-noise ratio sufficient to measure 10 fA beam current; some ideas taken from the electronics developed in REX-ISOLDE at CERN are currently under investigation. For less than 10 fA, a counting technique seems to be the only possibility.

8.6.3 Energy and time detector.

Two other important beam parameters (energy and bunch length) are not a big challenge at this very low intensity, because the same technique as currently used in ALPI could be used also for the SPES beam: MCP for timing structure and silicon detector for energy and longitudinal emittance measurements. A problem could be the time needed to gather meaningful information.

8.7 Vacuum System for SPES

In the framework of the SPES project, there are two main reasons which demand to renew the ALPI vacuum system completely. First of all, the circulating RNB species along the beam lines is a diffuse source of contamination which restricts the actual pump specifications. Secondly, in view of an experimental campaign of one to two decades with SPES beams, the pumps must be replaced due to their general significant ageing.

Although the actual level of vacuum is satisfactory to minimize beam losses (low 10^{-7} mbar range in warm conditions), the vacuum pumps must be anyway replaced, for operation in presence of radioactive contamination, because of the different requirement of maintainability. In fact, due to losses of radioactive beams and in case of acceleration of species of relatively long life time – or isotopes with long time decay process – the presence of radioactive contamination in the ALPI beam line should be very low, but the costs in terms of time and money increase. Not only additional safety precautions for personnel must be taken into account, but also procedures for waste storage and disposal must be carried out, to avoid further dispersion of radioactivity.

Thus, it is mandatory to choose pumping systems with high reliability, for minimal maintenance and with low waste production. Moreover, the control of contamination within these systems should be easy to inspect. While the magnetic turbo-pump is the high vacuum pump choice, dry sealed pumps must be preferred, as far as for roughing-vacuum or fore-vacuum pumping is concerned.

The present status of ALPI vacuum equipment – along with its control system – dates back to the early nineties. Both in ALPI cryostats and in diagnostic boxes, turbo-molecular pumps equipped with magnetic bearing, backed by rotary pumps with zeolite traps, are installed. The ALPI transfer lines towards the experimental halls make use of turbo-molecular pumps coupled with sputter-ion pumps for high vacuum. All the equipment has been almost in continuous operation since the installation, and only on the turbo-magnetic pumps a heavy maintenance was made after more than ten years of operation. This was due to a period of frequent power supply interruptions that broke many pump bearings: the latter were replaced, along with the rotors.

In the last year, vacuum equipment ageing was confirmed by an increasing rate of failures. Technical assistance suggested renewing the ALPI vacuum components so to guarantee their availability for long term steady operation.

Most of the obsolete pumping systems in ALPI are located in the beam transfer lines towards the experimental halls, downstream the junction between the TANDEM and ALPI exit lines. Most of the pumps (turbo, ionic, and rotary) in these lines were installed 30 years ago. Nowadays not only is their maintenance very costly, but the control system precludes the possibility of an automatic operation for setting, operating and monitoring the vacuum system. In late 2012, LNL decided to equip one of the experimental beam transfer lines (namely the one to the 8π LP-Experimental Station) with a completely new pumping system. The new layout foresees a combination of two turbo-molecular pumps with (250 l/s) backed by dry sealed pumps ($20 \text{ m}^3/\text{h}$) and two sputter ion pumps (110 l/s). The layout, shown in Figure 8.27, provides a lower than 2×10^{-8} mbar pressure, everywhere along the line (Figure 8.28).

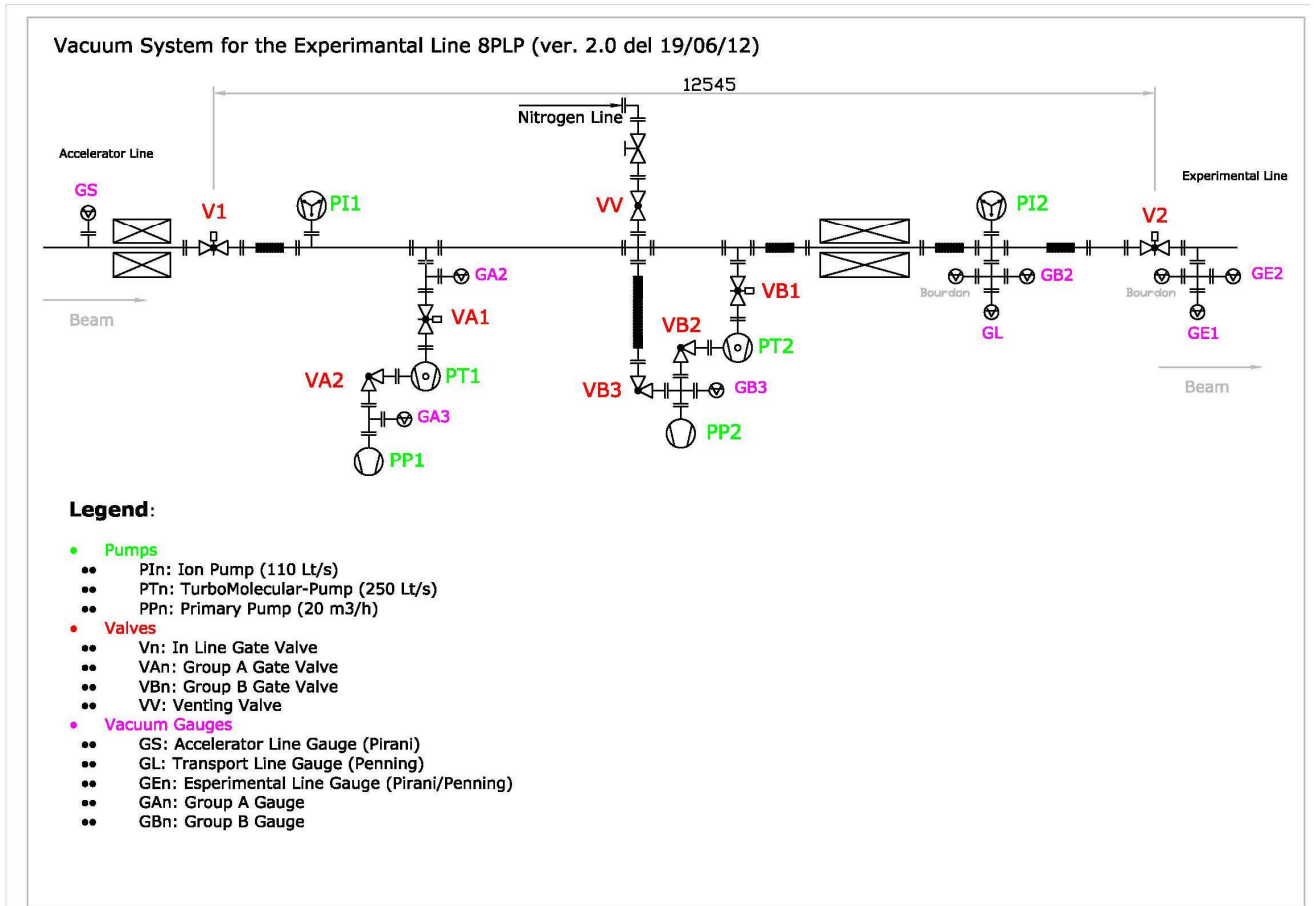


Figure 8.27: Vacuum System for the Experimental Line 8 π LP

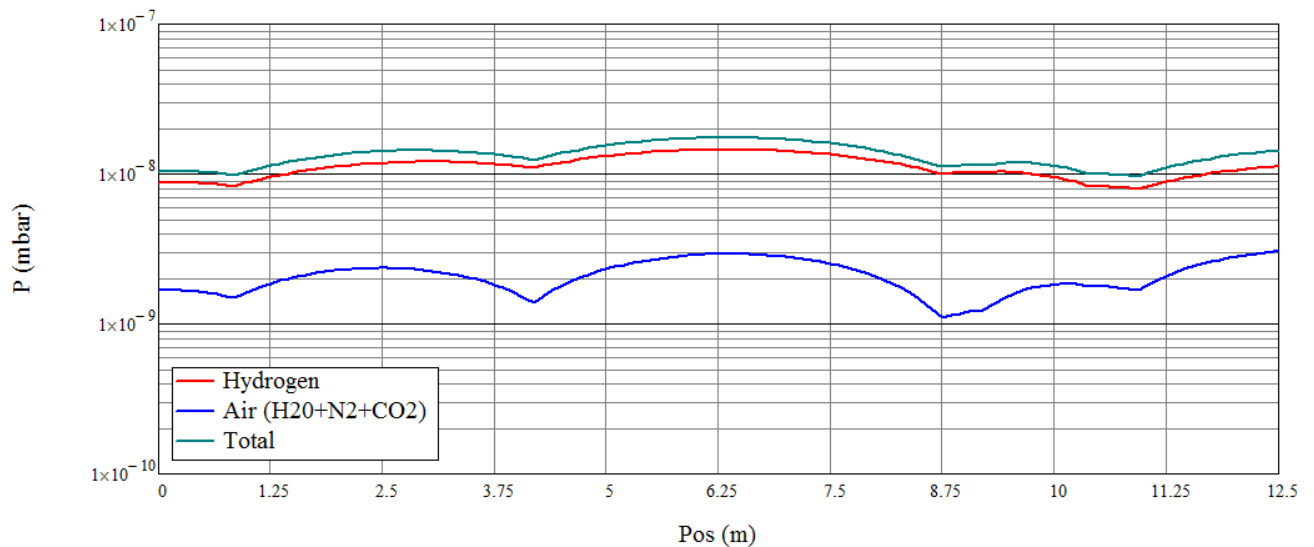


Figure 8.28: Vacuum Profile for the Experimental Line 8PLP

Although turbo-pumps equipped with magnetic bearing are virtually free of maintenance, to reduce the implementation costs, it is possible to choose pumps with ceramic bearings. As a drawback, maintenance is required every two years of continuous operation. Maintenance operations can be performed in house and lead to very small production of waste material.

The SPES vacuum system will be prototyped relying on this new prototype layout. The devices will be used as a standard for the new pumping station and will be used also for

prototyping the new vacuum control system. As soon as the upgrading of the 8π LP experimental channel will be completed, the new vacuum control system will be extended to all the remaining channels, and afterwards to all pumping stations in ALPI cryostats, diagnostic boxes and beam input and output lines, including those involved by the ALPI upgrade in the SPES project.

The new control system design is based on Siemens PLC, operating under EPICS supervision. The PLC will provide for the setting and the operation of all the vacuum devices (pumps, insulating valves and vacuum gauges) both in normal and emergency conditions. All the acquired data will be remotely available and stored on an EPICS-based server.

As a matter of fact, the reliability of the present ALPI control system is fairly good. However, it is based on unusual components built by an external company, which are now obsolete. It is then impossible to ensure long term operation or maintenance in case of component failure. The upgrade of the vacuum control system is hence a mandatory objective for a long term-use of the SPES facility. Not only does it increase the reliability of ALPI cryostats, but it is also important for safety considerations.

Concerning fore pumps and roughing pumps, their refurbishment is also mandatory, both in ALPI and in the experimental halls.

The necessity of conveying exhaust gas residues into a common storage shall be evaluated, according to the radioprotection requirements (being evaluated).

8.8 Upgrade and Refurbishment plan of the Cryogenic Plant of ALPI for SPES

At INFN-LNL three cryogenics plants are operational: 2 refrigerators, for the linac ALPI and PIAVE respectively, and one liquefier producing liquid He from gaseous He for various experiments (cavity tests, ultra-cryogenic antenna for gravitational wave detection, and others). The three plants share the gaseous He recovery system and some purification facilities.

The largest plant is devoted to the main linac (ALPI) [33] and will be in operational also for SPES, of which ALPI is the RNB accelerator. This plant is described quite in detail in Appendix I of this chapter (par. 8.11). The rest of the present chapter is dedicated to the upgrade measures, either completed or proposed in the SPES framework.

First of all, the already achieved upgrade of ALPI cryogenic power capability (from 700 to more than 1000 W) is described, which is a fundamental condition to be able to extend ALPI with 2 additional cryostats with Nb-Sputtered cavities, thus allowing a final energy of RN beams beyond 10 MeV/A to be achieved (par. 8.8.1).

Beyond the cryogenic power upgrade, several systems require – after more than two decades of operation – special measures: even nowadays the cryogenics of ALPI is subject to faults which require frequent interventions and often do not allow operation with the desired reliability. Some failures or problems cannot be solved with routine maintenance, but require special interventions.

In detail, special interventions should be targeted to the following subsystems (parr. 8.8.2 to 8.8.7):

- Cryostats control System
- Alpi refrigerator control system
- Layout of linac cryostats
- Valve box for helium cryogenic transfer lines
- Compressor units
- Recovery and purification system

8.8.1 ALPI Refrigerator Upgrade

The helium refrigerator of the superconducting ALPI accelerator was commissioned in 1991. It is manufactured by Air Liquide; it uses a Claude cycle processing up to 150 g/s of helium. It consisted of a Brayton cycle with two gas bearing turbines, also used to cool the thermal shields of the cryostats, and Joule-Thomson (JT) expansion valve or, as an alternative, a reciprocating wet expander (WE) for the liquid helium production. In 1991 the refrigerator was accepted, with the WE, giving a refrigeration power of 3900 W at 60-70 K plus 1180 W at 4.5 K. The use of the wet expander was abandoned soon due to its discontinuous stability of operation. The subsequent continuous operation with only the JT valve was just enough, in terms of refrigeration capacity to comply both for the shields and, at 4.5K, with the number of cavities and cryostats installed (~ 700 W). In 2008, it was proposed by LNL to install a third helium turbine as an alternative to the WE, in order to increase the limited refrigeration capacity at 4.5 K. The design of the supercritical turbine was assigned to Air Liquide.

According to the calculation carried out with a third turbine, processing up to 70 g/s of helium, 300÷400 W at 4.5 K can be added to the existing refrigeration capacity.



Figure 8.29: Photo of ALPI Cold Box, recently upgraded with a 3rd turbine.

Due to the higher priority of ALPI accelerator operation with respect to upgrades, the cryogenic system renewal was completed only in summer 2012. Fig. 8.29 shows ALPI cold box after the installation of the third turbine. Figure 8.30 shows the results in terms of refrigeration capacity at 4.5 K after the upgrade. A measured increase of 360 W, with respect to the previous JT configuration, can be observed.

Furthermore the refrigerator can process more helium gas, thus exceeding the 1100 W refrigeration capacity at 4.5K as shown.

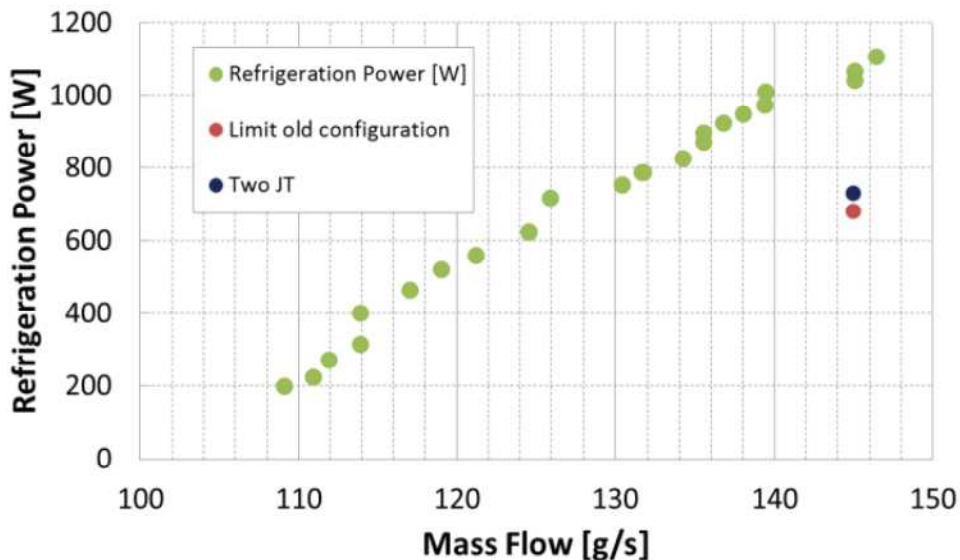


Figure 8.30: Refrigeration capacity available at 4.5 K after the installation of the supercritical turbine (green dots). The gain at 145 g/s, with respect to the previous configuration (red dot) is $(1040 - 680) = 360$ W. In the actual configuration, without T3 in operation, an additional capacity is anyway available, due the by-pass valve of T3 action as an additional isenthalpic expansion in series with the JT valve (blue dot).

The achieved result, in terms of refrigeration capacity, makes it possible to compensate for the additional 100W higher power dissipation, due to the cryostat reshuffling process proposed in the next paragraph, without losing refrigeration power redundancy.

8.8.2 *Urgent Upgrade of the Cryostats Control System*

At present, the cryostats control is realized as follows: each single cryostat has a dedicated controller (fig. 8.39) which is installed in a rack, together with all the remaining electronic equipment. Each single rack hosts 2 controllers, performing the cryogenic processes. These components are very old and can no longer be maintained.

All cryostats are then supervised by software, installed in 2 industrial PCs dating from the 90's, with the old and non-standard operating system QNX. Both the software and the PC are so old that no spares are available. A simple hardware failure or damage to a file system could compromise the functionality of the cryostats or the whole supervision system.

If a failure regarded the controller, only the related cryostat could become uncontrollable and should be kept off in the accelerator: that would simply decrease the final energy, unless the cryostats hosting bunching resonators were affected, in which case the whole linac would be unusable.

If, however, the supervision system would break down, no cryostat could be controlled and the operation of the entire linac would be impossible.

The first prototype of a new control system (fig. 8.31), based on standard and industrial PLC, is at present in the test phase. As soon as possible, a revised version of this prototype, to be extended to all controllers, will be realized, which should be the best compromise between functionality and cost.

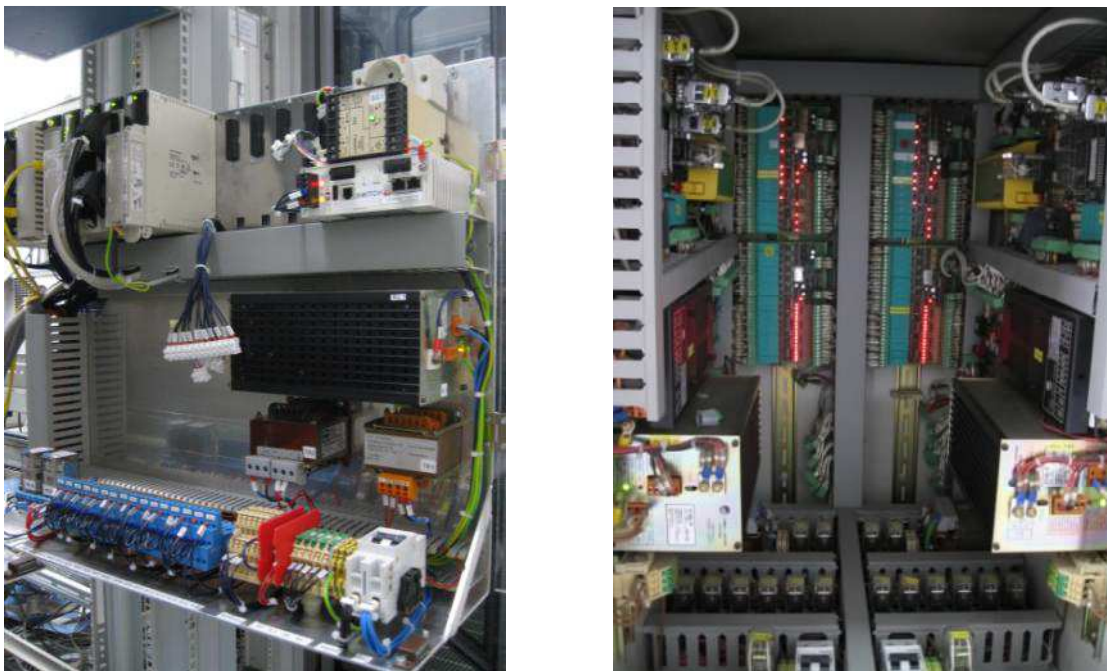


Figure 8.31: *New, PLC-based, cryostat control system and old cryostat controller*

8.8.3 *Complete refurbishment of Alpi refrigerator control system for SPES*

The ALPI refrigerator was built by Air Liquide as a prototype project, based on their standard refrigerator model “Helial”. The control system is an old PLC model, Eurotherm

PC3000 (fig. 8.32). This system is very old and the spare parts are no longer available. We have just a few spares in house at present.

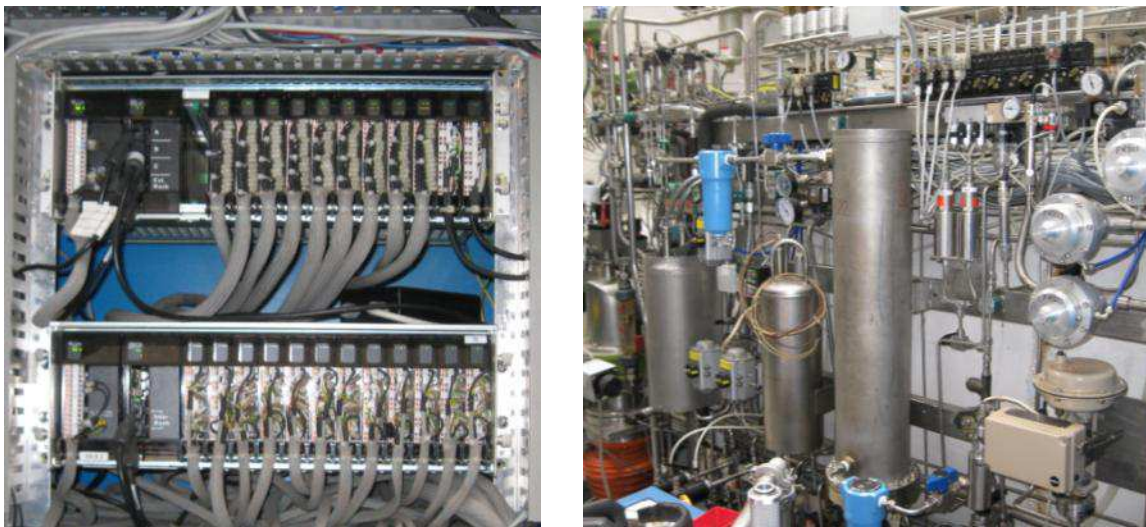


Figure 8.32: PLC Eurotherm and digital/analog modules of ALPI plant control system (left) Cold Box on-board components (right)

The risk of failure is large and the chance of a cryoplant fault, with no more spares for a swift restart, is increasing. Unless a new control system is rapidly designed and ordered, a fatal failure may imply at least 1 year stop of the plant and of the accelerator itself.

The revamping of the control system is a demanding task because this is a non-conventional plant and the cryogenic process shall have to be carefully studied and understood. The turbines, for example, which are the core of the plant, need a very complex control system.

We could follow one of the three following routes:

- the first and safest is also the most expensive: to purchase a new control system from Air Liquide;
- the second could be the realization of the revamping in house, by copying and writing step-by-step the old control code to be written into the new PLC;
- the third possibility is to adopt the UNICOS standard that is used at CERN to control all the cryogenic systems of LHC.

The 3rd option assumes that we may be supported by the CERN cryogenic team, at least in the implementation phase. Future maintenance and possible upgrades of a UNICOS-based system (internally or with external support) should be properly envisaged in this option too. This option might be attractive also from the point of view of the increase in proficiency of the local staff. It should be noted that, at present, the revamping of our small cryogenic helium liquefier (Linde TCF20 plant) is being finalized with UNICOS, under support from CERN experts.

8.8.4 *Change of the layout of linac cryostats in the SPES project*

The future configuration of ALPI will include the 2 additional cryostats, which are installed in PIAVE at present, and two additional cryostats on the high energy side (see par.8.5): they are marked in yellow in fig.8.33. They will have to be connected to the cryogenic lines.

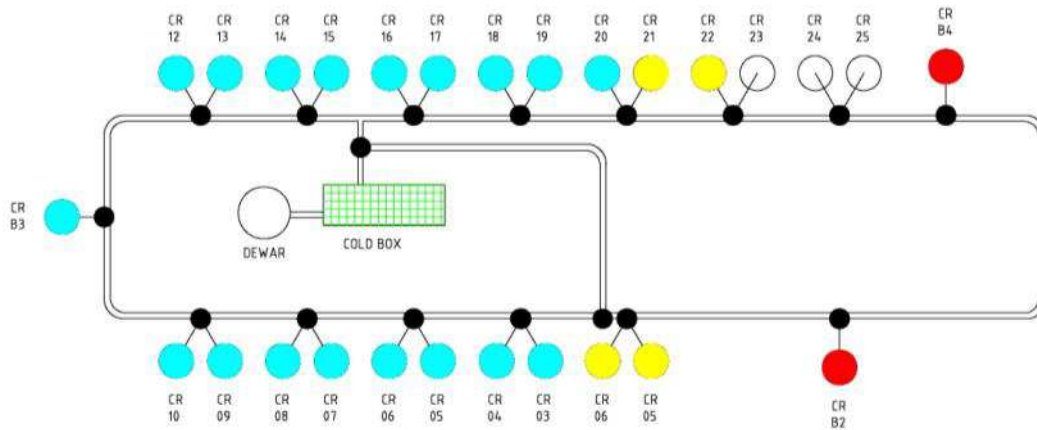


Figure 8.33: layout of ALPI cryostats – in yellow the modifications to the present layout

It will be necessary to modify and adapt the lines to arrange the space for the new cryogenic valve boxes, which perform the task of distributing liquid and gaseous He between the cold box and the cryostats.

Since the low energy cryostats use liquid nitrogen too, in order to refrigerate the cavity input couplers (see par. 8.4), connections with the existing liquid nitrogen distribution system shall have to be realized, by installing all the necessary equipment (sensors, cryogenic valves, flexible hoses).

New racks, where to install the new control system for the additional cryostats, shall also be required. In fact, the cryostats presently operating in PIAVE are monitored by the main PLC of the PIAVE refrigerator and it is not possible to separate their present control system (from both the software and hardware standpoints) from the main program. The new cryostat control system will be identical to that which has to be installed in the rest of the linac (see par. 8.8.4.1 above).

8.8.5 Valve boxes replacement

The valve boxes (fig. 8.34), installed along ALPI cryogenic transfer lines, are equipped with inner valves, which are totally inside the vacuum chamber and operate at cold temperatures.

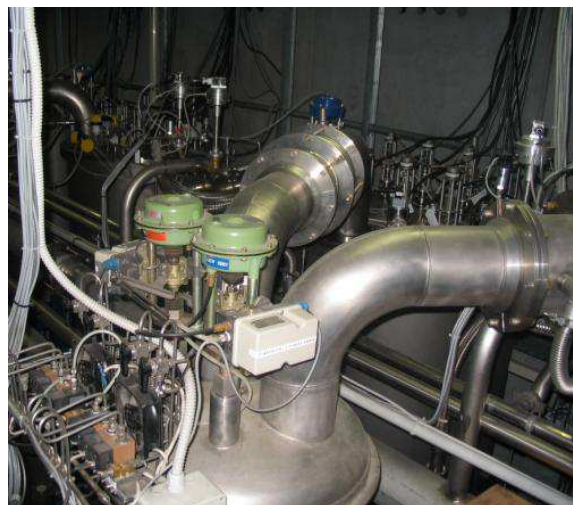


Figure 8.34: Valve box of linac cryogenic transfer line

Their only connection with the warm temperature side is a little pipe (6 mm diameter), which is used to activate the inner actuator, by applying 16 bars of gas helium. An advantage is that these valves have small dimensions and a reduced thermal leak.

If this valve, however, gets blocked during operation, or obstructed to such an extent that local warm up does not solve the problem, the only solution is to cut and open the vacuum tank of the valve box. In this specific case, only the related cryostat would be out of order, while the other cryostats would continue to be operational.

However, in case of a gaseous leak into the valve box vacuum chamber, the entire cryogenic transfer line would be vented and the whole line could not be operated: this would result in a long-term shutdown of the entire linac. For these reasons, in the SPES project framework, we think it is wise, at least, to design and realize at least 3 new valve boxes: 2 will be used for the cryostats to be added in the SPES layout, while the third one could be kept as spare part, ready to be installed in case of emergency. Of course, in the long run, the replacement of all valve boxes would be highly recommended (though quite expensive, on the SPES budget scale).

8.8.6 *Compressor Units Refurbishment*

The compression units provide the necessary helium mass flow to the Cold Box for the cryogenic process. ALPI features 3 compressor units and 4 screw compressors. A supervision control does not exist and, at the moment, compressors are operated without any chance to monitor the process remotely.

The compressors electrical power cabinets are 20 years old and their main components should be replaced.

The frames of the compressor units (see fig. 8.35), and one of them in particular, generate a high level of vibrations (of increasing amplitude) that tend to damage other components. System modifications must be investigated, so as to solve this problem.



Figure 8.35: *Compressor units C and D*

8.8.7 *Recovery and Purification System*

A number of very important refurbishments are required on this system, in order to increase the reliability of the entire ALPI cryogenic plant in the SPES project framework.

These refurbishments are motivated and explained hereinafter.

Refurbishment of the liquid nitrogen purifier.

Refrigerators, in particular conditions or during some of their processes, tend to lose gas helium that is generally recovered into the common “recovery system”. Dedicated compressors store it into high pressure vessels (up to 200 bars).

In order to refill the refrigerator with pure gas, and compensate for the above mentioned losses, it is necessary to clean it from contaminants (water and air, in particular). The purification process starts from the dryers (fig.8.36) where the water is removed at warm temperature. Then the cryogenic purifiers remove air.



Figure 8.36: Gaseous helium dryers

At LNL, a Liquid Nitrogen Purifier is employed upstream the specific cryogenic purifier of the cold box, essentially to clean the gas from air contamination. It is a standalone installation and, independently of the conditions of the cryoplants, it can provide pure helium gas. With this purifier, we avoid the risk of blocking or damaging the cryogenic purifiers of the refrigerators (fig. 8.37).



Figure 8.37: Internal purifier of ALPI refrigerator: damage, occurred in 2010 because of excessive water pollution, is visible

The LN2 purifier has been working for many years, but it is now suffering from frequent faults, interrupting the purification process. To guarantee more reliable working conditions, it is necessary to renew the control system and to replace the main components of the plants (as valves, actuators and pneumatic systems).

Refurbishment and Automation of the Recovery System

In order to have an adequate storage of pure helium gas for various purposes and needs (for example to accelerate the cryoplant start up or to reduce the risk of plant stop in case of problem with the purification systems) it is necessary to increase the capacity of pure helium, by adding a new tank (50 cubic meter) where to store the gas at warm temperature (fig. 8.38).

The recovery system storage consists in 32 vessels (fig. 8.39), each ones of 2 m³ capacity, with a maximum pressure of 200 bars. All vessels are connected in different groups, so as to make the required storage volume available, depending on the particular experimental conditions. These groups are put in line, in different modes which depend on the pressure conditions and on the operation mode of the cryoplants.



Figure 8.38: present buffer system for pure helium gas at INFN-LNL



Figure 8.39: “manual” control panel of the high pressure storage (left) and high pressure vessels (right)

The present control is fully manual, including valves (fig. 8.47). This creates management difficulties: in case of sudden evaporation of large quantities of liquid helium, a large free volume is required to store all the gas; in normal conditions, on the other hand, a continuous high pressure flow of helium is needed, to optimize the purification process. At the moment the operator is switching manually (and frequently) from a mode to another in order to cope with the changing operational modes.

The installation of a dedicated control system will handle the gas distribution, without requiring the presence of a dedicated operator. It will avoid

- the risk to lose gas helium in air, if the storage volume is insufficient,
- or
- the risk to contaminate/block the purifiers if the pressure is too low for the purification process.

8.9 Conclusions

All the main upgrades and refurbishment of the linac, which have been herein reviewed, will make ALPI a suitable accelerator of RNB species for long years ahead. SPES will join brand new installations (from the cyclotron driver to the new RNB injector into ALPI, passing through the target-ion-source, the beam cooler, the HRMS) with others (ALPI, transport lines, experimental lines) which are 20÷30 years old.

Concerning ALPI as an RNB accelerator, during the construction of the new injector (of which the ECR charge breeder and the RFQ are the main components) it is mandatory to continue the upgrade and refurbishment activity on ALPI, to optimize it for RNB beams, while retaining its capability for stable (and RNB-pilot) beams. Upgrade on cavity equipment and cryostats, both on the low and the high energy sides, is required to provide the required RNB energy (~10 MeV/A) with 90% transmission, for which an upgrade of the magnetic quadrupole lens gradients from 20 to 25 T/m might be an asset. The vacuum system must be renovated (both HW and SW) to make it suitable to handle potentially activated residues and as a consequence of its significant ageing. The cryogenic plant needs increase of the available power, so as to create the required redundancy and to refrigerate an increased number of cryostats; meanwhile, extraordinary maintenance on various systems will be conducted, in order to make it better manageable and to increase its availability. Last not least, ALPI diagnostics boxes, able at present to detect position, size, current, and energy-time features of higher current stable beams (nA scale), shall have to be equipped with instruments targeted to a fA÷pA current range (not straightforward and time-consuming developments, which had been launched well ahead of the project construction).

All above mentioned activity shall have to be conducted with the smallest possible interference with PIAVE and ALPI being used for physics with stable beams, during the foreseen 5 years of construction of the SPES facility.

8.10 References

1. CERN Accelerator School on Ion Sources, Senec (Slovakia) June 2012
2. I. G. Brown, *The Physics and Technology of Ion Sources*, 2nd ed. (Wiley-VCH, New York, 2004).
3. R. Geller, *Electron Cyclotron Resonance Ion Sources and ECR Plasma*, Institute of Physics, Bristol, 1996.
4. R. Geller et al, RSI 67 1281 (1996).
5. L. Spitzer Jr, *Physics of Sully Ionized Gases*, Dover Publication Inc.
6. R. Vondrasek et al, RSI 83 02A913 (2012).
7. T. Lamy et al, RSI 79 02A909 (2008).
8. T. Lamy et al, Proc. of the 20th International Workshop on Electron Cyclotron Resonance Ion Sources (ECRIS-2012), Sydney (Australia).
9. C. Barton et al, RSI 79 02A905 (2008).
10. F. Ames, RSI 81 02A903 (2010).
11. P. Delahaye et al, RSI 83 02A906 (2012).
12. TraceWin IRFU CEA, (<http://irfu.cea.fr/Sacm/logiciels/index3.php>)
13. F. Herfurth et al., AIP Conf. Proc. Vol. 793, pp 278-292 (2005).
14. M. Comunian, "Dinamica del fascio nell'RFQ del nuovo iniettore di ioni Pb al CERN", degree thesis, Padua University, 1994 (in italian)
15. K.R.Crandall et al., "PARMTEQ-A beam dynamics code for the RFQ linear accelerator, LA-UR-88-1546.
16. R. Duperrier, Phys. Rev. Vol.3, 124201(2000)
17. R. Ferdinand, Proceedings of PAC09, Vancouver (CA), 4281, <http://accelconf.web.cern.ch/AccelConf/PAC2009/papers/fr2gri02.pdf>
18. www.ansys.com
19. M. Comunian, Proc. of HIAT12, 136, <http://accelconf.web.cern.ch/AccelConf/HIAT2012/papers/tuc01.pdf>

20. D. Zenere et al., Proceedings of SRF2007, Peking Univ., Beijing, China, 450, <http://accelconf.web.cern.ch/AccelConf/srf2007/PAPERS/WEP08.pdf>
21. A. Facco, J.S. Sokolowski and B. Elkonin, Proc. of the 3rd European Particle Accelerator Conference, Berlin, 1992, vol.2, 1276.
22. A. Facco, F. Scarpa and V. Zviagintsev, Proc. of HIAT98, Argonne (Chicago, USA), 185.
23. A. Facco, Particle Accelerators, Vol. 61, 1998, 265-278.
24. A. Facco, V. Zviagintsev, R. Laxdal and E. Chiaveri, Proc. of PAC 2001, Chicago, USA, June 18-22, 2001, 1092
25. M. Marchetto, R. E. Laxdal, V. Zvyagintzev, Proc. of PAC 07, Albuquerque (NM, USA) 1392.
26. R. Poirier et al., Proc. of LINAC 2004, Lubeck (Germany), 228.
27. A.M. Porcellato et al., Proc. of HIAT12, Chicago (IL, USA), 73, <http://accelconf.web.cern.ch/AccelConf/HIAT2012/papers/po10.pdf>
28. S. Stark et al., Proc. of of SRF2007, Peking Univ., Beijing, China, 216
29. G. Bisoffi et al., Proc. of HIAT12, Chicago (IL, USA), 106, <http://accelconf.web.cern.ch/AccelConf/HIAT2012/papers/tua02.pdf>
30. http://spes.lnl.infn.it/%7Espes/TDR2008/Chapter3_performances.pdf, 50
31. J. L. Wiza, Nuclear Instruments and Method 162 (1979), 587
32. http://www.lnl.infn.it/%7Eannrep/read_ar/2002/index_2002.html, 259
33. R. Pengo et al., Cryogenics vol. 30, 1990, 74
34. R. Pengo et al., LNL-INFN [REP]. 13/1988 (Internal Report)

8.11 APPENDIX I - ALPI CRYOGENIC PLANT

ALPI cryogenic plant, built by Air Liquide, was commissioned around 20 years ago. It was designed for more than 1100 W of cryogenic power at 4,2K and around 3900 W at ~ 80K, though, for reasons which will be explained below, the cryogenic power at 4,2 has always been substantially lower (below 750 W in operation), a value which became rapidly marginal, towards the addition of new cryostats. With basically no cryogenic power redundancy, the stability of cryogenic parameters (pressure in the cryostats and along the transfer lines in particular) has always been an issue, and a limit to the availability of the plant and the linac itself.

In view of another couple of decades of its exploitation with SPES, important and urgent measures have to be taken, both to improve the plant performances and to refurbish those systems which most suffer from ageing and the replacement of which is mandatory for reliable operation.

In this chapter, the main constituents of the generic cryogenic plant will be briefly reviewed (par. 8.8.1); technical figures of the overall cryogenic systems at INFN-LNL (par. 8.8.2) and, more specifically, ALPI plant and its main constituents are given (par. 8.8.3). Finally, the upgrade and refurbishment measures – foreseen in the SPES project – are discussed (par. 8.8.4).

8.11.1 Ideal Cryogenic plant

An ideal cryogenic plant, used both for refrigeration and liquefaction modes, is illustrated in Figure 8.40. Typically, a reserve of gaseous helium (pure and less pure) and liquid is stored. Gaseous helium, after being purified if necessary, is compressed to 10÷20 bar and is subject to the thermodynamic processes required to transform it into liquid He. When gaseous helium is in a closed cycle between usage and compression systems, we have the “refrigeration” mode. In this process, ideally, the amount of helium is retained. When the gas is used in liquefaction systems (open cycle), losses are larger and helium purification, before usage, is required.

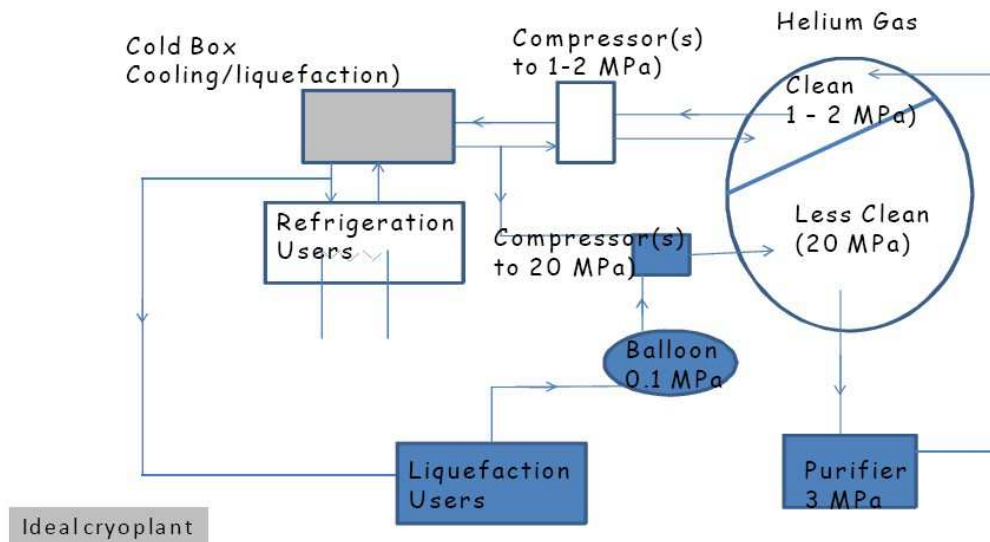


Figure 8.40: Scheme of an ideal cryoplant

8.11.2 Cryogenics at LNL

LNL cryogenic plants are shown schematically in Fig. 8.41. Its basic constituents are:

- 16 + 16 tanks for the less pure helium with maximum operating pressure of 200 bara.

- Tanks (buffers) for pure helium gas, each one dedicated to individual refrigeration/liquefaction plants
- Cryogenic purifier (2x30 m³/h), working with liquid nitrogen
- Cycle compressors of the cryoplants, working at nominal pressure of 10, 13, 16 bar for TCF20, TCF50, ALPI respectively
- Compression systems up to 200 bar for the recovery of evaporated helium
- Cold Boxes (CB), where transformations take place for the thermodynamic cooling/liquefaction of TCF20, TCF50 and ALPI
- System known as “Auxiliary Cold Box”, needed to that keep the heat shields of the cryostats cold (at 80K), in case of stop of ALPI cryoplant
- Another apparatus for gas recovery from different users

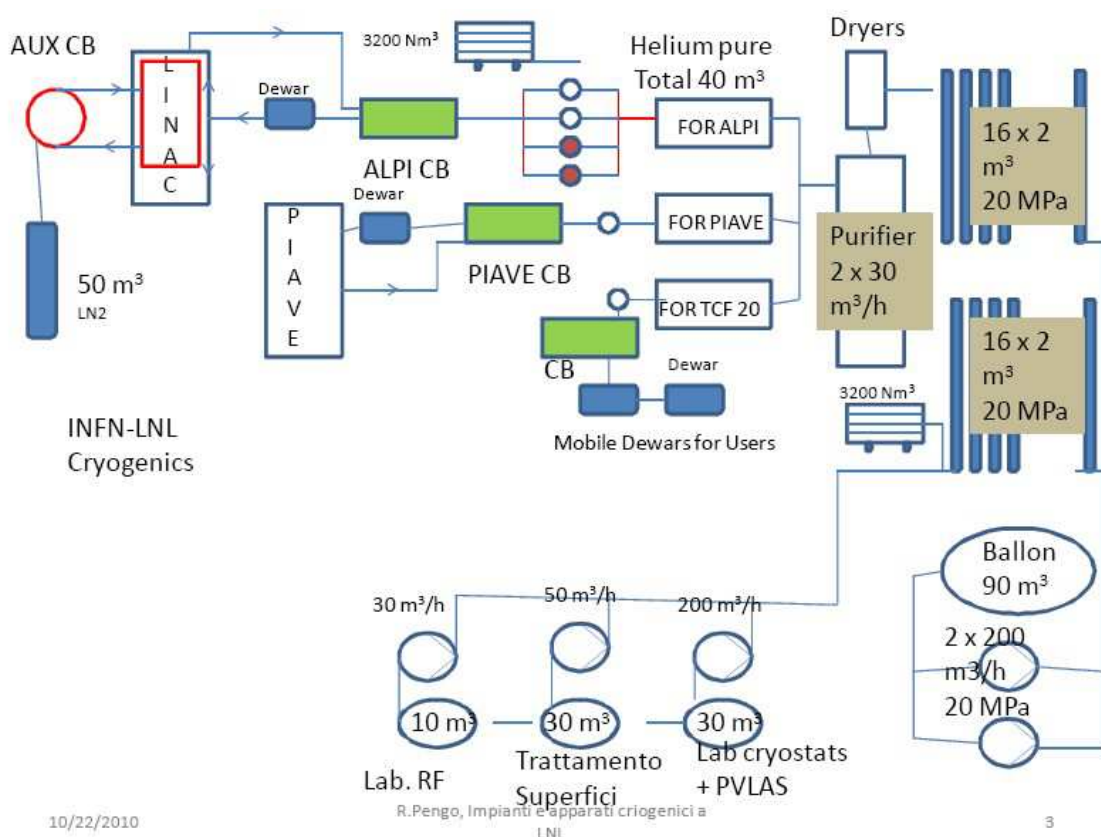


Figure 8.41: – cryogenic plants at LNL

8.11.3 Alpi Cryoplant

The cryogenic plant of ALPI has been realized to provide liquid helium and gaseous helium in a continuous mode. Occasionally, it may be also used for the production of liquid helium to refill mobile dewars (when liquid helium production exceeds what is required by the linac).

ALPI refrigerator was commissioned in the nineties for a cooling capacity of 1150 W at 4.5 K and 3900 W between 60 and 80 K. This was obtained with a Claude cycle consisting of two turbines in series and an expander piston, called "wet expander". The "wet expander" has never been used due both to technical difficulties and to the high level of mechanical vibrations which would shake the superconducting resonators, driving them off-lock; without it, the power was reduced to about 700W. Now, with the addition of a second JT (Joule Thomson) valve the power is increased by approximately 30÷50 W; with the additional 3rd turbine (fig. 8.42) the power is

increased by more than 300 W returning to the nominal power of 1150W. This was obtained with the same mass flow and, therefore, the same power consumption of cycle compressors.

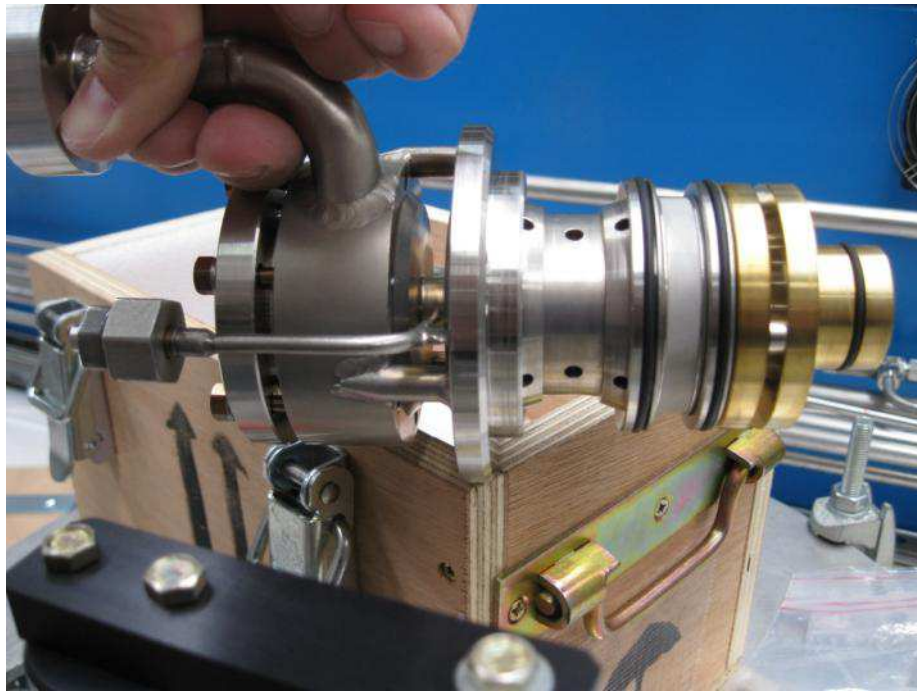


Figure 8.42: Third turbine of ALPI cryogenic system; it gives operational stability to the plant and allows adding a few cryostats on the beam line, as foreseen by the SPES layout

ALPI cryogenic system can be divided into four main subsystems:

1. Compression units (fig. 8.43)
2. Cold box (fig.8.44)
3. Cryogenic transfer lines (fig. 8.45)
4. Cryostats (fig. 8.46)
5. Auxiliary cold box (fig. 8.47)

8.11.3.1 Compression units

In the ALPI refrigerator, 4 compressors are installed, separated into three distinct units. Two units house two-stage screw Mycom compressors (fig. 8.43), with nominal mass flow 65 g / s (compressor A) and 95 g / s (compressor B) respectively, while the third unit hosts two-stage screw Howden compressors (compressor C and D), each with a mass flow of 55 g / s.

Each unit is independent with respect to the circuits of lubrication oil, heat exchanger oil/water and gas/water and the whole control system (PLC and sensors).



Figure 8.43: screw compressor of ALPI-SPES cryogenic plant

8.11.3.2 The Cold Box

The Cold Box is the part in which the compressed gas is allowed to expand and cool down until it reaches the liquid conditions and becomes a liquid-vapor mixture. Inside the Cold Box (fig 8.44) several heat exchangers are installed, through which heat is exchanged between the hot inlet gas and the cold evaporated gas coming back from the distribution lines. One of the most important components of the system is the cryogenic turbine, which expand the gas by extracting energy and transferring it outside.

In ALPI, 3 turbines are installed. The third one was installed in summer 2012, thus increasing the overall power by more than 300 W @ 4.2 K.

Liquid helium is collected in a phase separator (a dewar). From there, the liquid is sent, through the cryogenic transfer lines, to the cryostats.



Figure 8.44: ALPI Dewar and Cold Box

8.11.3.3 Cryogenic Transfer Lines

Liquid helium (4K @ 1,3 bara), gaseous helium (60K and 80K @ 7 bara line) and liquid nitrogen (78 K @ 1,5 bara) are transported through special lines, called cryogenic lines, constructed so as to minimize the thermal load from environment. In ALPI there are ~110 meters of lines connecting the Cold Box to the 20 cryostats, through 10 valve boxes.

In each valve box (for 2 cryostats) the following valves are installed: 1 control valve for liquid helium and 3 on/off valves (return liquid line at 5K, and supply and return gas lines at 60÷80K). The on/off valves are fully inside the vacuum tank and are very complicated to maintain.

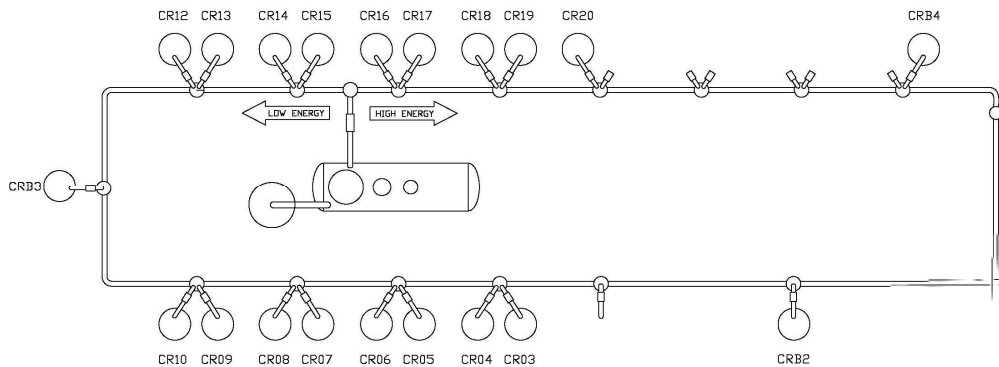


Figure 8.45: Present layout of ALPI cryogenic transfer line

8.11.3.4 Cryostats

In ALPI, 20 cryostats housing 74 superconducting quarter wave resonators are installed [34].

Cryostats are connected to the cryogenic lines, providing helium and liquid nitrogen. Each cryostat is equipped with ~20 silicon-diodes temperature sensors, to monitor the thermal conditions of the superconducting cavities and the lines. A superconducting liquid helium probe and the pressure transmitters supervise the liquid helium circuits.

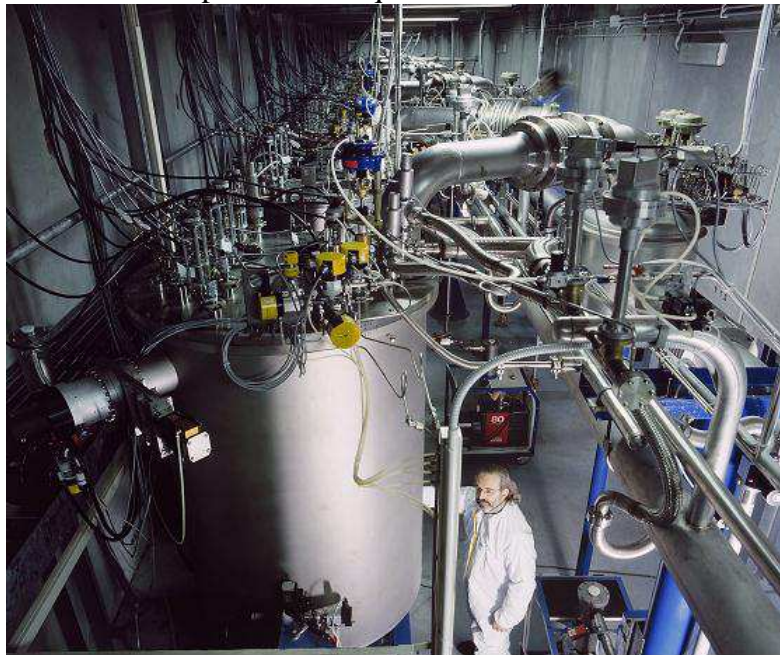


Figure 8.46: Cryostats in ALPI linac; tubes connecting the valve box to cryostats are visible in the foreground

8.11.3.5 Auxiliary Cold Box

The auxiliary cold box was installed, in order to keep the heat shields of the cryostats housing the superconducting cavities cold, in case of plant stop (for example electrical power shutdown). It consists of two helium circulators of 100 g/s gas flow each, sending helium gas ($\Delta P = 0.5$ bar) to the shields, after it has been cooled in a heat exchanger immersed in a bath of liquid nitrogen. The operation cost of the auxiliary CB, in terms of consumption of liquid nitrogen, is lower than the (electrical) cost for the operation of the compressor B alone, required to provide the 95 g/s flow that would keep the cryostat shields cold with gaseous He.

The Auxiliary cold Box can provide 6000 W@ 80K, 7 bara.



Figure 8.47: installation of the heat exchanger in the Auxiliary Cold Box

